Vglut2-based glutamatergic signaling in central noradrenergic neurons is dispensable for normal breathing and chemosensory reflexes

Author names and affiliations

Yuan Chang[1], Savannah Lusk[2], Russell Ray[1,2,3,4]

[1]Department of Molecular Physiology and Biophysics, Baylor College of Medicine, Houston TX

[2]Department of Neuroscience, Baylor College of Medicine, Houston TX

[3]McNair Medical Institute, Houston TX

[4]Corresponding author, russell.ray@bcm.edu

Abstract

Central noradrenergic (NA) neurons are key constituents of the respiratory homeostatic network. NA dysfunction is implicated in several developmental respiratory disorders including Central Congenital Hyperventilation Syndrome (CCHS), Sudden Infant Death Syndrome (SIDS) and Rett Syndrome. The current unchallenged paradigm in the field, supported by multiple studies, is that glutamate co-transmission in subsets of central NA neurons plays a role in breathing control. If true, NA-glutamate co-transmission may also be mechanistically important in respiratory disorders. However, the requirement of NA derived glutamate in breathing has not been directly tested and the extent of glutamate co-transmission in the central NA system remains uncharacterized. Therefore, we fully characterized the cumulative fate maps and acute adult expression patterns of all three Vesicular Glutamate Transporters (*Slc17a7* (Vglut1), *Slc17a6* (Vglut2), and *Slc17a8* (Vglut3)) in NA neurons, identifying a novel dynamic expression pattern for Vglut2 and an undescribed co-expression domain for Vglut3 in the NA system. Our functional studies showed that loss of Vglut2 throughout the NA system failed to alter breathing or metabolism under room air, hypercapnia, or hypoxia in unrestrained and conscious mice, which demonstrates that Vglut2-based glutamatergic signaling within the central NA system is not required for normal baseline breathing and hypercapnic, hypoxic chemosensory reflexes. These outcomes challenge the current understanding of central NA neurons in the control of breathing

and suggests that glutamate may be not a critical target to understand NA neuron dysfunction in respiratory diseases.

Introduction

Breathing is a vital and life-sustaining function supporting homeostatic processes, most critically maintaining blood pH/CO_2 and O_2 levels within a narrow physiological range. Respiratory homeostasis is mediated by neuron-modulated lung ventilation adjustments in response to physiological deviations resulting in high pCO_2 or low pO_2 blood and tissue levels, known as the hypercapnic and hypoxic reflexes respectively (Del Negro et al., 2018; Dick et al., 2018). These reflexes are part of a complex brainstem neural network that integrates a multitude of information streams across the central and peripheral nervous systems to regulate respiratory output. Within this brainstem network, central noradrenergic (NA) neurons are known to be an important component that plays a variety of roles in modulating breathing. Furthermore, various perturbations across the central NA system have been implicated in several developmental disorders with respiratory and chemosensory features such as Central Congenital Hyperventilation Syndrome (CCHS), Sudden Infant Death Syndrome (SIDS) and Rett Syndrome (Beltrán-Castillo et al., 2017; Feldman et al., 2013; Gauda et al., 2007; Viemari, 2008). Thus, understanding how central NA neurons modulate respiratory chemoreflexes or chemosensory breathing is critically important for the development of new diagnostic and therapeutic interventions to address respiratory pathophysiology.

Central noradrenergic neurons are commonly thought to exert their effect on breathing through their primary neurotransmitter noradrenaline and adrenaline. However, in addition to noradrenaline, several studies suggest that glutamate is co-transmitted in subsets of central NA neurons. Vesicular glutamate transporter 2 (Vglut2), a gene marker of glutamatergic signaling, has been shown to be co-expressed in subsets of central NA neurons including, C1/A1, C2/A2, A5, and LC in adult rats and mice (DePuy et al., 2013; Souza et al., 2022a; Stornetta et al., 2002a, 2002b; Yang et al., 2021), though NA specific expression of related Vglut1 and Vglut3 transporters remains unknown. Additionally, it has been well documented that central NA

58 neurons co-expressing Vglut2 innervate key respiratory centers, such as preBötzinger complex
59 and parafacial region (pFRG), as well as many other autonomic brainstem and forebrain centers
60 that could indirectly drive a change in breathing if perturbed, i.e., cardio-vascular function, the
61 intermediolateral nucleus (IML)-sympathetic system and metabolism (Supplemental table 1).
62 Thus, it has currently become a dominant paradigm in the field of respiratory physiology that NA-
63 based glutamate release is a critical form of neurotransmission in the control of breathing. This
64 paradigm is supported by multiple papers. Abbott et al. (2014) showed that Vglut2 is required for
65 an increase in respiratory rate when anterior C1 neurons are unilaterally opto-genetically
66 stimulated. Malheiros-Lima et al. (2020) showed that Vglut2-expressing C1 neurons project to
67 the pFRG region, and hypoxic breathing was blunted after blockade of ionotropic glutamatergic
68 receptors at the pFRG site in anesthetized rats, together supporting a role for anterior C1 neurons
69 releasing glutamate at the pFRG site in turn to regulate breathing under hypoxia. Similarly,
70 Malheiros-Lima et al. (2022) and Malheiros-Lima et al. (2018) showed that Vglut2-expressing C1
71 neurons project to the NA A5 region and the preBötzinger complex respectively, and again the
72 blockade of ionotropic glutamatergic receptors at the A5 region or preBötzinger complex reduced
73 the increase in phrenic nerve activities or in respiratory frequency elicited by optogenetic
74 stimulation of C1 cells in an anesthetized preparation. In addition, Guyenet et al. (2013) and
75 others speculate that the apparent lack of plasmalemmal monoamine transporter in C1 fibers
76 indicates reduced or absent noradrenergic or adrenergic signaling due a lack of re-uptake and
77 neurotransmitter pool depletion (Comer et al., 1998; Lorang et al., 1994). Cumulatively, the
78 studies argue for glutamate as the predominant functional neurotransmitter for C1 NA neurons
79 in the breathing neural network. To our knowledge, this dominant perspective has not been
80 otherwise previously challenged. Although these studies are informative, the evidence
81 supporting the role of NA-based Vglut2 signaling in respiratory control are either indirect and
82 circumstantial or cannot be seen as physiological given experimental limitations, such as the focal
83 nature of opto-genetic stimulation. Thus, it is not yet clear what the requirement is for NA-based
84 glutamatergic signaling in homeostatic breathing in the awake and unrestrained animal and how
85 that might inform upon disease.
86

87 To better understand the role of NA-based glutamatergic signaling in breathing, we sought to
88 both fully characterize the molecular profiles of the central noradrenergic system with respect to
89 glutamate co-expression and to determine the requirement of Vglut2-based glutamatergic
90 release in respiratory control under physiological chemosensory challenges in awake and
91 unrestrained mice. We first fully characterized the recombinase-based cumulative fate maps for
92 Vglut1, Vglut2 and Vglut3 expression and compared those maps to their real time expression
93 profiles in central NA neurons by RNA *in situ* hybridization in adult mice. We found a novel
94 dynamic expression pattern for Vglut2 and an entirely undescribed co-expression domain for
95 Vglut3 in the central NA system. Secondly, to determine if Vglut2-based glutamatergic signaling
96 in NA neurons is required for respiratory homeostasis, we conditionally ablated Vglut2 in all NA
97 neurons and tested respiratory, chemosensory, and metabolic function in unrestrained and
98 conscious mice. Using the same genetic model in prior studies (Abbott et al., 2014), conditional
99 deletion of Vglut2 in NA neurons did not significantly impact breathing under room air,
100 hypercapnic, or hypoxic conditions. These results demonstrate, for the first time, that NA Vglut2-
101 based glutamatergic signaling is dispensable for respiratory control, which challenges the
102 prevalent perspective on the role of C1 and other Vglut2 expressing NA neurons in respiratory
103 homeostasis and suggests that glutamate may not be a critical target to understand NA neuron
104 dysfunction in respiratory diseases.
105
106 **Results**
107 **Cumulative fate maps of central noradrenergic neurons co-expressing Vglut1, Vglut2 and**
108 **Vglut3**
109 To fully characterize the expression profiles of all three glutamate markers Vglut1, Vglut2 and
110 Vglut3 in central noradrenergic neurons, we first used an intersectional genetic strategy (Figure
111 1A). We bred three Cre drivers *Slc17a7*^{Cre} (Vglut1-Cre), *Slc17a6*^{Cre} (Vglut2-Cre) and *Slc17a8*^{Cre}
112 (Vglut3-Cre) to *Dbh*$^{p2a\text{-}Flpo}$ (DBH-p2a-Flpo) (targeting noradrenergic neurons) mice respectively.
113 The three compound lines of Vglut1-Cre/+; DBH-p2a-Flpo/+, Vglut2-Cre/+; DBH-p2a-Flpo/+, and
114 Vglut3-Cre/+; DBH-p2a-Flpo/+ were then crossed with the *Rosa26*$^{RC::FLTG}$ (RC::FLTG) intersectional
115 reporter mice which express tdTomato in cells expressing only flippase (Flpo) while expressing

116 eGFP in cells co-expressing both Flpo and Cre recombinases. Thus, in each of the three
117 intersectional reporter crosses [e.g. 1) Vglut1-Cre/+; DBH-p2a-Flpo/+; RC::FLTG/+, 2) Vglut2-
118 Cre/+; DBH-p2a-Flpo/+; RC::FLTG/+ and 3) Vglut3-Cre/+; DBH-p2a-Flpo/+; RC::FLTG/+], NA
119 neurons without any Vglut1/2/3 expression are labelled by red fluorescent protein (tdTomato)
120 while NA neurons co-expressing either Vglut1, Vglut2, or Vglut3 are labeled by green fluorescent
121 protein (eGFP). By using this method, we characterized and quantified the expression profiles of
122 all three vesicular glutamate transporters Vglut1, Vglut2 and Vglut3 across every NA nucleus in
123 adult mice including A7, Locus Coeruleus (LC), sub CD/CV, A5, and throughout the anterior -
124 posterior dimension of C1/A1, C2/A2 (Figure 1B-D). Vglut1-Cre was not co-expressed in any
125 central NA nuclei in adult mice. However, Vglut2-Cre and Vglut3-Cre both showed co-expression
126 in central NA neurons. Vglut3-Cre-expressing NA neurons are restricted to posterior C2/A2 and
127 posterior C1/A1, and the majority is in posterior C2/A2 where 26.9 $\pm$ 3.16% NA neurons are
128 Vglut3-Cre positive. In posterior C1/A1, only 1.26 $\pm$ 0.559% NA neurons are Vglut3-Cre positive.
129 Surprisingly, 84.6 $\pm$ 3.75% NA neurons in total have Vglut2-Cre co-expression and each NA
130 nucleus was predominantly labelled by Vglut2-Cre expression. The percentage of Vglut2-Cre
131 positive NA neurons in A7, LC, A5, sub CD/CV, anterior and posterior part of C1/A1, anterior and
132 posterior part of C2/A2 is 69.8 $\pm$ 8.29%, 80.5 $\pm$ 3.78%, 84.8 $\pm$ 11.3%, 51.5 $\pm$ 2.61%, 99.0 $\pm$ 0.681%,
133 95.7 $\pm$ 2.40%, 96.1 $\pm$ 1.98%, 97.8 $\pm$ 0.771%, respectively (Mean $\pm$ SEM). The presence of Vglut2-
134 Cre co-expression in anterior NA groups was unexpected as previous *in situ* data in adult rats
135 found Vglut2 positive NA neurons only in the posterior C2/A2 and C1/A1 (DePuy et al., 2013;
136 Stornetta et al., 2002a, 2002b). Notably, however, the Vglut2 co-expression in the LC region
137 agrees with Yang et al. (2021) which also showed that a high percentage of LC NA neurons are
138 Vglut2 positive by using another intersectional strategy in mice, *Th^{Flpo}; Slc17a6^{Cre}; Rosa26^{Ai65}* (TH-
139 Flpo; Vglut2-Cre; Ai65). The differences in our and other fate maps compared to *in situ*
140 hybridization may either reflect early gene expression that is down regulated in the adult or may
141 reflect low levels of expression not detectable by *in situ* hybridization but that are nonetheless
142 sufficient to effect recombination in the intersectional genetic strategy.
143

144 **Real time mRNA expression patterns of Vglut1, Vglut2 and Vglut3 in central noradrenergic**
145 **neurons in adult mice**
146 DePuy et al. (2013), Stornetta et al. (2002a) and Stornetta et al. (2002b) showed that Vglut2 co-
147 expression is only located in the C2/A2 and C1/A1 region in the adult rat but not in anterior NA
148 nuclei in the brainstem by *in situ* hybridization. To verify if the real time NA-based Vglut2
149 expression pattern in adult mice is the same as in adult rats and to further characterize the
150 expression patterns of the other two vesicular glutamate transporters (Vglut1 and Vglut3) in
151 adult mice, we performed fluorescent RNA *in situ* hybridization experiments. We co-stained
152 Vglut1, Vglut2, Vglut3 with DBH respectively in brain tissue of adult mice and characterized the
153 colocalization of Vglut1/2/3 with DBH in brainstem NA nuclei A7, LC, A5, sub CD/CV, anterior
154 C1/A1 and C2/A2, and posterior C1/A1 and C2/A2 (Figure 2A-C). No Vglut1/DBH double positive
155 neurons were detected in any part of the central NA system, consistent with our fate map. Vglut3
156 mRNA colocalization with DBH is only found in the posterior part of C2/A2 where 27.1 $\pm$ 1.86%
157 DBH positive neurons have Vglut3 co-localization, again consistent with our fate map. For Vglut2,
158 we only found detectable levels of Vglut2 mRNA in C1/A1 and C2/A2 NA region, but not in A7,
159 LC, A5, sub CD/CV. Quantitatively, the percentage of Vglut2/DBH double positive neurons in
160 anterior C1/A1, anterior C2/A2, posterior C1/A1 and posterior C2/A2 is 84.7 $\pm$ 5.82%, 66.3 $\pm$
161 0.335%, 35.7 $\pm$ 3.01% and 90.1 $\pm$ 2.45%, respectively. This result is consistent with the previous
162 *in situ* data in adult rats (DePuy et al., 2013; Stornetta et al., 2002a, 2002b) suggesting that there
163 is no obvious expression difference of Vglut2 in the central NA system between mouse and rat.
164 However, the Vglut2 *in situ* data did not show expression in anterior NA populations. This
165 difference between our *in situ* data and fate map data supports our previous hypothesis that
166 many NA neurons expressed Vglut2 at some point from early development toward adulthood
167 but the expression of Vglut2 is turned back down during adulthood. Interestingly, Yang et al.
168 (2021) did show adult Vglut2 co-expression in LC by a viral injection of both Cre and Flpo-
169 dependent eYFP into the LC of a bi-transgenic mouse with both TH-Flpo and Vglut2-Cre. To verify
170 this result, we injected an AAV virus containing Cre-dependent tdTomato (pAAV-EF1a-DIO-
171 tdTomato-WPRE) into the LC region of adult Vglut2-Cre mice. Consistent with Yang et al. (2021),
172 we observed sparse Vglut2-Cre and TH (immunopositive) double positive neurons in the LC

173 (Figure 2 supplement 1). Additionally, Souza et al. (2022a) showed about 28.5% A5 neurons are
174 Vglut2 mRNA positive in adult rats by RNA scope, a method which is more sensitive than the
175 traditional *in situ* hybridization we used here. These data suggest that some adult NA neurons in
176 LC and A5 have Vglut2 co-expression, but the Vglut2 mRNA level cannot be detected by
177 traditional *in situ* hybridization.
178
179 **Vglut2 expression is effectively knocked down in the whole central noradrenergic system in**
180 **DBH-Cre; Vglut2 cKO mice**
181 To investigate the requirement of Vglut2-based glutamatergic signaling in the central NA system
182 in breathing under physiological challenges, we used Dbh-Cre; *Slc17a6*$^{flox/flox}$ (DBH-Cre; Vglut2
183 cKO) as the mouse model in which Vglut2 is inactivated in all noradrenergic neurons. This is the
184 same model used by Abbott et al. (2014) to show that Vglut2 expression in the NA system was
185 required for a modest increase in respiratory frequency following unilateral optogenetic
186 stimulation of anterior C1. To verify if Vglut2 expression is effectively removed from central NA
187 neurons in DBH-Cre; Vglut2 cKO mice, we carried out fluorescent RNA *in situ* hybridization for
188 Vglut2 and DBH in the mouse brainstems and compared the Vglut2 signal intensity in DBH
189 positive neurons in DBH-Cre; Vglut2 cKO and its littermate controls. We found that Vglut2 mRNA
190 expression is 96.4 $\pm$ 0.226% decreased compared to controls, indicating that the Vglut2 is
191 effectively recombined to abrogate expression in NA neurons (Figure 3A-B).
192
193 **Vglut2-based glutamatergic signaling in central NA neurons is not required for baseline**
194 **breathing nor for the hypercapnic ventilatory reflex under distinct CO_2 challenges**
195 Multiple prior studies provide indirect evidence that NA glutamate transmission may play roles
196 in respiratory function, particularly that anterior C1 neurons mediate the hypoxic ventilatory
197 response through the pFRG/RTN and/or the NA A5 group (Malheiros-Lima et al., 2022, 2020).
198 Additionally, the A5 group has been implicated in the hypercapnic reflex (Haxhiu et al., 1996).
199 Thus, we sought to determine if Vglut2-based glutamatergic signaling in central NA neurons is
200 necessary to regulate baseline breathing and the hypercapnic chemoreflex in awake and
201 unrestrained animals. We used whole-body barometric plethysmography to measure the

202 breathing and metabolism of conscious and free-moving mice. After a five-day habituation
203 protocol, the ventilation response of DBH-Cre; Vglut2 cKO mice and their littermate controls was
204 measured under room air and hypercapnia (5% CO_2) (Figure 4A). Surprisingly, DBH-Cre; Vglut2
205 cKO mice didn't show significant differences in overall respiratory output (V_E/V_{O2}), respiratory
206 rate (V_f), tidal volume (V_T), minute ventilation (V_E) and metabolism demand (V_{O2}) compared to
207 their littermate controls under both room air and 5% CO_2 challenge (Figure 4B and Table 1-2).
208 These results suggested that Vglut2-based glutamatergic signaling is not required for regulating
209 baseline breathing and hypercapnic ventilatory reflex under 5% CO_2.
210
211 To further investigate if Vglut2-based glutamatergic signaling in central NA neurons is required
212 for ventilation response of higher CO_2 challenges, we also measured the breathing of DBH-Cre;
213 Vglut2 cKO mice under 7% CO_2 and 10% CO_2. We found that under the 7% CO_2 condition, DBH-
214 Cre; Vglut2 cKO mice showed only a significantly decreased tidal volume (V_T), but the overall
215 respiratory output (V_E/V_{O2}), respiratory rate (V_f), minute ventilation (V_E) and metabolism demand
216 (V_{O2}) didn't show a significant difference between the mutant mice and their sibling controls
217 (Figure 5A-B and Table 3). This result suggests that Vglut2-based glutamatergic signaling in
218 central NA neurons is not required or at least is not as important as previously expected for
219 regulating the hypercapnic ventilatory reflex under 7% CO_2.
220
221 Under 10% CO_2 challenge, none of the overall respiratory outputs (V_E/V_{O2}), respiratory rate (V_f),
222 tidal volume (V_T), minute ventilation (V_E) and metabolism demand (V_{O2}) were significantly
223 different between DBH-Cre; Vglut2 cKO mice and their littermate controls, suggesting that
224 Vglut2-based glutamatergic signaling in central NA neurons is not required for the hypercapnic
225 ventilatory reflex under 10% CO_2 (Figure 6A-B and Table 4).
226
227 **Vglut2-based glutamatergic signaling in central NA neurons is not required for the hypoxic**
228 **ventilatory reflex under 10% O_2**
229 To determine if Vglut2-based glutamatergic signaling in central NA neurons is necessary to
230 regulate the hypoxic chemoreflex, we measured the ventilation response of DBH-Cre; Vglut2 cKO

231 mice under 10% O_2. We analyzed the five respiratory parameters in three 5-min time periods
232 under 10% O_2 challenge. No significant difference was found in the overall respiratory output
233 (V_E/V_{O2}), respiratory rate (V_f), tidal volume (V_T), minute ventilation (V_E) and metabolism demand
234 (V_{O2}) between DBH-Cre; Vglut2 cKO mice and controls in either of the three 5-min 10% O_2 periods
235 (Figure 7A-B and Table 5). These data suggest that Vglut2-based glutamatergic signaling in central
236 NA neurons is not required for the hypoxic ventilatory reflex under 10% O_2.
237
238 **Discussion**
239 Neuron co-transmission of two or more neurotransmitters across excitatory, inhibitory, and
240 neuro-modulatory facets is becoming an increasingly appreciated phenomenon in the central
241 nervous system. Functional interrogation of co-transmission is essential not only to understand
242 the distinct and cooperative roles that multiple signaling molecules may play at the synapse but
243 also to determine the most critical targets for potential therapeutics. To our knowledge, the
244 unopposed paradigm in the field until now has been that vesicular glutamate transporter 2
245 (Vglut2)-based glutamate transmission from central noradrenergic neurons is important in
246 respiratory homeostasis. Anatomically, it has long been appreciated that central NA neurons co-
247 express Vglut2, the major glutamate marker among three glutamate transporters (DePuy et al.,
248 2013; Souza et al., 2022a; Stornetta et al., 2002a, 2002b; Yang et al., 2021). Also, it has been well
249 documented that NA Vglut2 positive fibers innervate known central respiratory centers or other
250 autonomic centers, that, when perturbed, could disrupt respiratory homeostasis (Supplemental
251 Table 1). Functionally, multiple reports have argued that Vglut2-based glutamate transmission
252 plays a role in respiratory homeostasis. It has also been suggested that, at least for C1 neurons,
253 the apparent lack of a plasmalemmal monoamine transporter may attenuate or eliminate
254 noradrenergic or adrenergic release from these fibers. However as discussed below, much of the
255 functional evidence supporting a role for Vglut2-based glutamate transmission from central
256 noradrenergic neurons is circumstantial or of a non-physiological nature, and absent or
257 attenuated release of adrenaline and noradrenaline has not been demonstrated. Nonetheless,
258 the dominant perspective that NA-Vglut2 glutamate transmission plays a role in breathing has
259 remained unchallenged. Our studies here uncover a novel dynamic expression pattern for Vglut2

260 and an entirely undescribed co-expression domain for Vglut3 in the central NA neurons, and in
261 contrast to prior work, our results show that loss of Vglut2 in NA neurons does not appreciably
262 change baseline or chemosensory breathing in conscious and free-moving mice.
263
264 Vglut2 has been shown to be co-expressed in subsets of central NA neurons, however, to our
265 knowledge, the potential for the central NA neurons to express the other glutamate transporters
266 Vglut1 or Vglut3 has not been reported at the anatomical level. To determine if central NA
267 neurons express either Vglut1 or Vglut3 and to confirm the Vglut2 expression, we carried out
268 cumulative intersectional fate mapping using Vglut1-Cre/+; DBH-p2a-Flpo/+; RC::FLTG/+, Vglut2-
269 Cre/+; DBH-p2a-Flpo/+; RC::FLTG/+ and Vglut3-Cre/+; DBH-p2a-Flpo/+; RC::FLTG/+ compound
270 mouse lines. As this approach maps the cumulative history of expression, we also examined acute
271 adult expression of Vglut1, Vglut2 and Vglut3 using fluorescent RNA *in situ* hybridization. Our *in*
272 *situ* results for Vglut2 agreed with earlier published outcomes (DePuy et al., 2013; Stornetta et
273 al., 2002a, 2002b) showing as much as 80% expression in posterior NA neurons. However, there
274 was no appreciable signal in anterior groups (A7, LC, A5, sub CD/CV). This lack of expression was
275 in stark contrast to the cumulative fate map for Vglut2, showing as much as 75% of the anterior
276 central NA neurons were recombined by the Vglut2-Cre over the lifetime of the animal. To further
277 interrogate the acute activity of the Vglut2-Cre in the Locus Coeruleus in the adult mouse, we
278 injected a Cre responsive virus in LC of Vglut2-Cre mice. The outcomes from the cumulative fate
279 map and acute injections are in agreement with published results from Yang et al. (2021).
280 Notably our use of the DBH-p2a-Flpo avoided expression in the PBN that was seen in the TH-Flpo
281 mouse. In addition, 28.5% A5 neurons were shown to be Vglut2 positive in adult rats by RNA
282 scope (Souza et al., 2022b). It is notable that both our lab and work published by (DePuy et al.,
283 2013; Stornetta et al., 2002a, 2002b) failed to detect Vglut2 expression in anterior groups, but
284 that apparently very low levels can be detected by more sensitive recombinase and RNA scope
285 methods. Additional electrophysiological evidence suggests that this expression is functional
286 (Yang et al., 2021). Our data suggests that Vglut2 co-expression in anterior NA groups is time
287 dependent, though the underlying temporal dynamics of Vglut2 remain unknown. It is notable
288 that we see nearly 80% of the LC and 85% of A5 recombined in the intersectional strategy

representing lifetime expression, but our and other studies find only 20% of the LC and 28.5% of A5 may be expressing Vglut2 at any given moment in adults. This suggests either a temporal restriction in expression as the animal matures or may reflect dynamic change driven by behavioral or physiological experiences.

For Vglut1, neither fate map nor *in situ* hybridization revealed any co-expression within the central NA system. However, Vglut3 expression was found in the posterior part of NA neurons including C2/A2 and C1/A1, which is first characterized by this study. The majority of this Vglut3 co-expression is restricted to the posterior part of the C2/A2 NA population. This NA region has not been heavily implicated in respiratory control nonetheless it readily lends itself to interrogation by intersectional genetic methods and *in situ* hybridization. Given its distal expression from anterior C1, it is unlikely that Vglut3 would compensate for loss of Vglut2 in anterior C1, though this has not been ruled out. Further, while Vglut3 is a marker of glutamatergic neurons, its role in neurotransmission is not wholly defined as Vglut3 is typically found in soma and dendrites (Fremeau et al., 2004).

Based on the Vglut2 co-expression in NA neurons and their projections to multiple brain regions important in respiration, several studies suggest that glutamate in NA populations is important in breathing control. Those studies provide a mix of circumstantial, indirect, or limited evidence for the potential role of Vglut2-based glutamatergic signaling in central NA neurons in breathing regulation. However, it has not yet been shown whether or not NA-based Vglut2 signaling is required for respiratory control due to experimental caveats or limitations.

Abbott et al. (2014) showed that conditionally knocking out Vglut2 in the whole central NA system attenuated a modest increase in respiratory rate resulting from unilateral C1 optogenetic stimulation. Absolute values and other respiratory parameters, including tidal volume (V_T) and minute ventilation (V_E) were not reported, making direct comparison difficult. While the optogenetic stimulation did drive a Vglut2 dependent increase in respiratory rate, it is not clear if the resulting change in breathing reflects a native feature of the network that might be engaged

318 in chemosensory responses, exercise, or volitional control. Thus, it remains possible that strong
319 optogenetic stimulation of a small, isolated population drives a Vglut2 dependent but ectopic
320 function that is not typically engaged in the normal operation of the breathing network. Such
321 ectopic outcomes could come from several potential, non-exclusive mechanisms. First, unilateral
322 stimulation could drive a network hysteresis or dysregulation akin to a focal injury that is not a
323 typical biological feature (Ducros et al., 2003). This point is well made in Abbott et al. (2013) in
324 their discussion of C1 optogenetic stimulation where they state, "resulting cardiorespiratory
325 response pattern should not be considered strictly "physiological," because a physiological
326 response is never initiated by selective activation of a single cluster of CNS neurons and the
327 various subsets of C1 neurons are presumably never recruited en bloc under any physiological
328 condition". Second, strong stimulation could result in overwhelming synaptic mechanisms (i.e.,
329 glial uptake) resulting in glutamate spillover and unintended cross talk to affect extra-synaptic
330 neurons proximal to targeted NA fibers. Activity dependent spillover transmission has been
331 documented elsewhere in the nervous system (Henneberger et al., 2020; Hülsmann et al., 2000).
332 Third, the outcomes could be secondary to a different autonomic or behavioral function requiring
333 NA-derived glutamatergic signaling involving metabolism or circulation (DePuy et al., 2013; Yang
334 et al., 2021).
335
336 More circumstantially, Malheiros-Lima et al. (2020) suggested C1 neurons potentially release
337 glutamate at the pFRG site to regulate breathing under hypoxia by providing three indirect lines
338 of evidence: 1) Vglut2-expressing C1 neurons project to the pFRG region; 2) Increased breathing
339 was blunted after blockade of ionotropic glutamatergic receptors at the pFRG site under
340 anesthesia using chemical hypoxia; 3) Depletion of C1 neurons eliminated the increased
341 breathing elicited by hypoxia. However, 1) the glutamatergic signaling targeting the pFRG region
342 is not necessarily from C1 NA neurons since glutamatergic neurons from other regions also
343 project to the pFRG site (Yang and Feldman, 2018).Thus, it is possible that the glutamatergic
344 signaling that is required for hypoxic response is derived from other glutamatergic neurons such
345 as the preBötzinger complex and the RTN itself; 2) C1 neuron depletion knocks out all the

346 signaling modalities in the C1 population including both noradrenaline and glutamate. It is not
347 clear which signaling drives the hypoxic response.
348
349 Similarly, Malheiros-Lima et al. (2022) and Malheiros-Lima et al. (2018) showed that Vglut2-
350 expressing C1 neurons project to the NA A5 region and the preBötzinger complex respectively.
351 The blockade of ionotropic glutamatergic receptors at the A5 region or preBötzinger complex
352 reduced the increase in phrenic nerve activities or the breathing frequency caused by
353 optogenetic stimulation of C1 cells in anesthetized preparation. Together these results suggest
354 that Vglut2-expressing C1 neurons communicate with A5 or preBötzinger complex neurons by
355 releasing glutamate in turn to regulate phrenic nerve activities or breathing frequency. Again,
356 these two studies showed that C1 neurons are important to regulate phrenic nerve activities or
357 breathing frequency, however, it is not necessarily through a direct C1-A5 or C1-preBötzinger
358 complex glutamatergic pathway, whereas an indirect multi-synaptic pathway originating with C1
359 noradrenaline and ending with glutamate transmission from an intermediate to A5 or
360 preBötzinger complex cannot be ruled out. Importantly, in all four studies noted here, respiratory
361 measurements were limited or proxies of breathing under anesthesia were used. The role of NA-
362 Vglut2 signaling was not reported in the context of an awake, unrestrained animal under
363 normoxic, hypoxic, or hypercapnic breathing.
364
365 Thus, the limitations and indirect lines of the evidence in these studies raised the question as to
366 whether or not glutamatergic signaling in central NA neurons is required or necessary to
367 modulate respiratory homeostasis under more physiologically relevant circumstances and if NA-
368 derived glutamate is an important mechanism to understand the pathophysiology of NA neurons
369 in respiratory diseases. The goal of our study was to test the requirement of NA-based
370 glutamatergic signaling in breathing homeostasis in the awake and unrestrained animal under
371 conditions that would engage the whole respiratory control network rather than a singular
372 component that may drive hysteresis or artifactual outcomes. Our *in vivo* breathing data under
373 room air, hypoxic, and multiple hypercapnic conditions failed to show the requirement of NA-
374 derived Vglut2 in normal breathing and respiratory chemoreflexes directly. To ensure a rigorous

375 and robust conclusion, first we use exactly the same mouse model, DBH-Cre; Vglut2 cKO, as
376 Abbott et al. (2014) used, and confirmed, by a second method (fluorescent RNA *in situ*
377 hybridization) that Vglut2 expression was indeed abrogated in the whole central NA system. Our
378 results are in strong agreement with DePuy et al. (2013) that recombination is efficient. Notably,
379 we assayed for expression at the cell body, rather than the fibers and see no singular cell body
380 that is scored positive. Second, we measured the breathing of conscious, unrestrained, and
381 habituated mice under physiological challenges including normoxia, hypercapnia and hypoxia.
382 Third, multiple respiratory and metabolic parameters were measured and reported in absolute
383 values including respiratory rate, tidal volume, minute ventilation, oxygen consumption, overall
384 respiratory output (minute ventilation normalized to oxygen consumption) in order to visualize
385 breathing function comprehensively. Fourth, our experimental design was overpowered (i.e.,
386 n=16-21 vs 5-13 needed for power based on power analysis and n=7-8 reported in other
387 manuscripts). Each respiratory/metabolic parameter for each physiological condition including
388 room air, hypercapnia, and hypoxia was derived by quantifying the entire respiratory trace and
389 analyzed between mutant and sibling controls by using a powerful linear mixed-effects
390 regression model with animal type (experimental vs. control) as fixed effects, animal ID as a
391 random effect and including sex as a variable (there was no sex specific effect) (Lusk et al., 2022).
392
393 Despite our experimental design and the extensive nature of our measurements, there remain
394 several considerations in the interpretation of our data. First, we uncovered a novel NA co-
395 expressed glutamate transporter, Vglut3. It remains a formal possibility that Vglut3 somehow
396 compensates for the loss of Vglut2, however we argue that this is unlikely for the following
397 reasons. First, our model is the same used in the other study where an effect was seen with
398 optogenetic stimulation. Second, focus has been on anterior C1 whereas Vglut3 is expressed in
399 the posterior CA domains. Another consideration is that pre- or post-natal developmental
400 compensation corrects for the loss of NA derived glutamate. Again, we argue that is not likely, as
401 we are using the same adult model that provided the most direct evidence and first functionally
402 demonstrated a potential role for C1-derived glutamate in breathing. Second, Abbott et al.
403 (2014) highlight that Vglut2 negative NA neurons showed no obvious abnormalities in number,

404 morphology, and projection patterns. Third, we have examined the requirement of NA-expressed
405 Vglut2 in P7 neonate mice in the auto-resuscitation reflex and saw no differences (data not
406 shown). However, this could be better tested by using the Dbh-CreERT2 (DBH-CreERT2)
407 (Stubbusch et al., 2011) to more acutely remove Vglut2 expression (though this leaves a window
408 of 2-3 weeks for compensation to occur). Yet another consideration in interpreting our results is
409 that we only address the loss of NA-Vglut2 based signaling across the entire NA system. It remains
410 a formal possibility that we have removed Vglut2 dependent signaling from two counter
411 balancing regions of the NA system and are therefore left with null results whereas removal from
412 anterior C1 alone would show a requirement. To test this possibility, it would require an
413 intersection conditional approach, something that has not yet been shown to be efficient and
414 effective and would be beyond the scope of these studies. Additionally, in our studies, we
415 account for potential metabolic changes that may underlie or be coordinate with changes in
416 breathing. However, in this study we did not test for potential changes in blood pressure or other
417 autonomic functions as well as affective state that may, in some obscure way, compensate for
418 changes in breathing. Lastly, our results are loss of function in nature. We do not test sufficiency
419 or gain of function and cannot fully rule out a role for NA-Vglut2 based glutamatergic signaling in
420 the control of breathing.
421
422 From a translational perspective, our data questions whether or not glutamatergic signaling in
423 NA neurons is likely to be a key mechanism and therefore a therapeutic target for breathing
424 disorders, such as Rett syndrome and SIDS. *Mecp2*-deficient mice (a mouse model of Rett
425 Syndrome that phenocopies many human symptoms) showed both a deficiency of NA
426 populations (reduced number of NA neurons in C2/A2 and C1/A1 group) and highly variable
427 respiratory rhythm at around 4-5 weeks of age (Roux et al., 2007; Viemari et al., 2005). 80% Rett
428 Syndrome patients experience breathing issues, such as unstable breathing, episodes of
429 hyperventilation and breathing holds, during the whole lifespan including both childhood and
430 adulthood (Ramirez et al., 2020). SIDS decedents show NA abnormalities and are hypothesized
431 to ultimately succumb from a failure in cardiorespiratory autoresuscitation (Chigr et al., 1989;
432 Garcia et al., 2013; Kopp et al., 1993; Mansouri et al., 2001; Ozawa et al., 2003; Takashima and

433 Becker, 1991). However, DBH-Cre; Vglut2 cKO mice, have normal baseline and chemosensory
434 respiratory parameters as adults and neonate mice show normal autoresuscitation indicating
435 that perturbed NA based glutamatergic signaling may not be a key driver in these or other related
436 respiratory pathophysiologies.
437
438 In conclusion, our studies demonstrated the extent of glutamate as a functional vesicular
439 glutamate transporter co-expression in central noradrenergic system. We were able to
440 characterize a novel Vglut3-expressing NA population in the posterior C2/A2 nuclei and found a
441 different Vglut2 co-expression pattern in anterior NA groups from a cumulative intersectional
442 fate map compared to a viral fate map and *in situ* hybridization in the adult, suggesting that
443 anterior NA populations may have a time-dependent or experience-dependent manner for
444 Vglut2 expression. Furthermore, despite prior studies providing indirect and circumstantial
445 evidence that noradrenergic-based glutamatergic signaling may play a role in control of
446 breathing, our studies that remove Vglut2 expression from noradrenergic neurons failed to
447 perturb room air breathing, the hypercapnic ventilatory reflex, and the hypoxic ventilatory reflex,
448 which challenges the current dominant perspective and provides further insight into the
449 potential role of NA-glutamate transmission in the control of breathing. Based on our data, we
450 suggest that noradrenergic-based glutamatergic signaling is not required for regulating baseline
451 breathing or the hypercapnic and hypoxic respiratory chemoreflexes, and glutamate may not be
452 a critical mechanistic component of NA neuron dysfunction in respiratory disorders.
453
454 **Materials and Methods**
455 **Ethical Approval**
456 Studies were approved by the Baylor College of Medicine Institutional Animal Care and Use
457 Committee (IACUC) under protocol AN-6171, and all experiments reported here were performed
458 in accordance with relevant guidelines and regulations.
459
460 **Breeding, Genetic Background, and Maintenance of Mice**

461 We maintained all our heterozygous mouse strains by backcrossing to wildtype C57BL/6J mice
462 and homozygous mouse strains by sibling crosses. For immunofluorescence experiments,
463 heterozygous B6;129S-*Slc17a7*$^{tm1.1(cre)Hze}$/J (*Slc17a7*^{Cre}, Vglut1-Cre) (Jax Stock No: 023527),
464 *Slc17a6*$^{tm2(cre)Lowl}$/J (*Slc17a6*^{Cre}, Vglut2-Cre) (Jax Stock No: 016963) *and* B6;129S-
465 *Slc17a8*$^{tm1.1(cre)Hze}$/J (*Slc17a8*^{Cre}, Vglut3-Cre) (Jax Stock No: 018147) were mated with
466 heterozygous *Dbh*$^{em2.1(flpo)Rray}$ (*Dbh*$^{p2a\text{-}Flpo}$, DBH-p2a-Flpo) (MMRRC ID: 41575) (Sun and Ray, 2016)
467 mice respectively to derive compound lines with both Cre and Flpo alleles (Vglut1-Cre/+; DBH-
468 p2a-Flpo/+, Vglut2-Cre/+; DBH-p2a-Flpo/+, and Vglut3-Cre/+; DBH-p2a-Flpo/+). Then these three
469 compound lines were each mated with homozygous B6.Cg-*Gt(ROSA)26Sor*$^{tm1.3(CAG\text{-}tdTomato,\text{-}}$
470 $^{EGFP)Pjen}$/J (*Rosa26*$^{RC::FLTG}$, RC::FLTG) (Jax Stock No: 026932) to derive three different intersectional
471 mouse lines Vglut1-Cre/+; DBH-p2a-Flpo/+; RC::FLTG/+, Vglut2-Cre/+; DBH-p2a-Flpo/+;
472 RC::FLTG/+ and Vglut3-Cre/+; DBH-p2a-Flpo/+; RC::FLTG/+. For *in situ* hybridization experiments,
473 wildtype C57BL/6J mice were ordered from the Center of Comparative Medicine (CCM), Baylor
474 College of Medicine. For NA-Vglut2 conditional loss of function *in situ* hybridization and
475 plethysmography experiments, hemizygous transgene Tg(Dbh-cre)KH212Gsat (Dbh-Cre, DBH-
476 Cre) (MMRRC ID: 036778-UCD GENSAT) mice were mated with homozygous *Slc17a6*^{tm1Lowl}/J
477 *(Slc17a6*$^{flox/flox}$*)* (Jax Stock No: 012898) to derive Dbh-Cre; *Slc17a6*$^{flox/+}$. Dbh-Cre; *Slc17a6*$^{flox/+}$ mice
478 were mated with *Slc17a6*$^{flox/flox}$ to derive Dbh-Cre; *Slc17a6*$^{flox/flox}$ (DBH-Cre; Vglut2 cKO). Sibling
479 mice that lacked the Cre allele or carried the Cre allele but lacked the floxed Vglut2 alleles were
480 used as controls. Rosa26 specific primers for the RC::FLTG mice were 5'-
481 GCACTTGCTCTCCCAAAGTC, 5'-GGGCGTACTTGGCATATGAT, and 5'-CTTTAAGCCTGCCCAGAAGA
482 (Ray et al., 2011) and yield a 495 bp band (targeted) and 330 bp band (wt). Cre-specific primers
483 for all Cre drivers were 5'-ATCGCCATCTTCCAGCAGGCGCACCATTGCCC and 5'-
484 GCATTTCTGGGGATTGCTTA and yielded a 550 bp band if positive. Flpo-specific primers for DBH-
485 p2a-Flpo are 5'- CACGCCCAGGTACTTGTTCT and 5'-CCACAGCAAGAAGATGCTGA (Sun and Ray,
486 2016) and yielded a 226 bp band if positive. *Slc17a6*^{flox} specific primers for Vglut2-floxed mice are
487 available at The Jackson Laboratory website (https://www.jax.org/strain/012898).
488
489 **Immunofluorescence staining**

490 Vglut1, Vglut2, or Vglut3-Cre/+; DBH-p2a-Flpo/+; RC::FLTG/+ adult mice were sacrificed and
491 transcardially perfused with 0.1 M phosphate-buffered saline (PBS) then with 4%
492 paraformaldehyde (PFA) in PBS. Mouse brains were dissected out and fixed for 2h in 4% PFA
493 before a PBS rinse and dehydration in 30% sucrose in PBS. Brains were embedded in OCT blocks,
494 sectioned at the thickness of 30µm, mounted on slides, and stored at -80°C until they were ready
495 for staining. The slides were hydrated in 0.1% Triton-X in PBS (PBST) for 15 mins, blocked with 5%
496 donkey serum in 0.1% PBST for 1h at room temperature and then incubated with primary
497 antibodies for 72 hours at 4°C in 0.1% PBST with 5% donkey serum. Tissues were washed in 0.1%
498 PBST 3 times for 10 min each and then incubated with secondary antibodies for 2hs at room
499 temperature in 0.1% PBST with 5% donkey serum. Slides were washed with 0.1% PBST for 10 min
500 and washed in PBS twice for 10 min each, stained for DAPI, washed 3 times for 10 min each with
501 PBS and mounted in ProLong Glass (Invitrogen). The following primary and secondary antibodies
502 were used: chicken anti-GFP (1:1,000, Abcam ab13970), rabbit anti-dsRed (1:1,000, Clontech
503 632496), donkey anti-chicken Cy2 (1:500, Jackson 703-225-155), donkey anti-rabbit Cy3 (1:500,
504 Jackson 711-165-152).
505
506 **In situ hybridization**
507 Mouse brains were dissected out from adult mice with 6-8 week of age, sectioned into
508 25µm brain sections and mounted on slides. We generated a digoxigenin (DIG)-labeled
509 mRNA antisense probe against Vglut1, Vglut2, and Vglut3 and fluorescein (FITC)-labeled mRNA
510 against DBH using reverse-transcribed mouse cDNA as a template and an RNA DIG or FITC-
511 labeling kits from Roche (Sigma). Primer and probe sequences for the Vglut1, Vglut2, Vglut3 and
512 DBH probes are available in the Allen Brain Atlas (http://www.brain-map.org). For the Vglut2 and
513 DBH double ISH in DBH-Cre; Vglut2 cKO and their littermate controls, we generated a new Vglut2
514 probe targeting exon 2 of Vglut2 specifically (Tong et al., 2007) and the probe sequence is 892-
515 1144bp as Slc17a6 transcript variant 1 and the size is 253bp. ISH was performed by the RNA In
516 Situ Hybridization Core at Baylor College of Medicine using an automated robotic platform as
517 previously described (Yaylaoglu et al., 2005) with modifications of the protocol for double ISH.
518 Modifications in brief [see Yaylaoglu et al. (2005) for buffer descriptions]: both probes were

519 hybridized to the tissue simultaneously. After the described washes and blocking steps the DIG-
520 labeled probes were visualized using tyramide-Cy3 Plus (1/75 dilution, 15-minute incubation,
521 Akoya Biosciences). After washes in TNT, the remaining HRP-activity was quenched by a 10-
522 minute incubation in 0.2M HCl. The sections were then washed in TNT, blocked in TNB for 15
523 minutes, and incubated at room temperature for 30 minutes with HRP-labeled sheep anti-FITC
524 antibody (1/500 in TNB, Roche/Sigma). Following washes in TNT, the FITC-labeled probe was
525 visualized using tyramide-FITC Plus (1/50 dilution, 15-minute incubation, Akoya Biosciences).
526 Following washes in TNT, the slides were stained with DAPI (invitrogen), washed again, removed
527 from the machine, and mounted in ProLong Diamond (Invitrogen).
528
529 **Viral Injection**
530 To verify Vglut2 co-expression in LC in adult mice (Yang et al., 2021), 6-week-old Vglut2-Cre mice
531 were injected with pAAV-EF1a-DIO-tdTomato-WPRE virus (RRID:Addgene_133786, obtained
532 from Joshua Ortiz at the Optogenetics and Viral Vectors Core at the Jan and Dan Duncan
533 Neurological Research Institute, 1ul at 7.90E+10 Gc/mL) into the LC (coordinates from bregma
534 anteroposterior −5.4 mm, lateral + 0.8 mm and dorsoventral – 4.0 mm) and allowed to incubate
535 for 4 weeks.
536
537 **Plethysmography**
538 Plethysmography on conscious and free-moving mice was carried out as described in (Ray et al.,
539 2011) on 6-8-week-old adult animals with at least 16 animals in both the experimental and
540 control group for each experiment. Animals were subjected to a five-day habituation protocol
541 with each day including several minutes of handling, temperature taken by rectal probe and at
542 least 30 min exposure in the plethysmography chamber (Martinez et al., 2019). Plethysmography
543 was then performed for each mouse within 1 week of the last day of habituation. On the day of
544 testing, mice were taken out from their home cage, weighed, and rectal temperature was taken.
545 Animals were then placed into a flow-through, temperature-controlled (about 32°C with real-
546 time temperature recording) plethysmography chamber and allowed to acclimate for at least 45
547 min in room air (21% O_2/79% N_2) conditions. After acclimation and measurement under room

548 air, the chamber gas was switched to a hypercapnic or hypoxic mixture of 5% CO_2/21% O_2/74%
549 N_2, 7% CO_2/21% O_2/72% N_2, 10% CO_2/21% O_2/69% N_2, or 10% O_2/90% N_2, depending on the
550 protocol, for 20 min. Chamber gas was then switched back to room air for another 20 min. The
551 animals were removed from the chamber and rectal temperature was measured immediately
552 after the mice were taken out from the chamber.
553
554 **Plethysmography data analysis and statistics**
555 Details were previously described in (Martinez et al., 2019; Ray et al., 2011). Plethysmography
556 pressure changes were measured using a Validyne DP45 differential pressure transducer, CD15
557 carrier demodulator and a reference chamber, and were recorded with LabChart Pro in real time.
558 Respiratory waveforms were analyzed by the BASSPRO module of the Breathe Easy software to
559 determine respiratory frequency (V_f), tidal volume (V_T), minute ventilation (V_E), oxygen
560 consumption (V_{O2}) and ventilatory equivalents for oxygen (V_E/V_{O2}) (Lusk et al., 2022). A power
561 analysis was performed using the reported effect size in Abbott et al. (2014) which used the same
562 mouse model as we used here and 5-13 mice were necessary to observe a statistically significant
563 result (Abbott et al. (2014) was able to see a significant difference between two groups with n=7
564 mice). In our experiments, the sample size for each group (DBH-Cre; Vglut2 cKO and control)
565 exceeded 13. Results (V_f, V_E, V_T, V_{O2}, V_E/V_{O2}) for room air and hypercapnic or hypoxic data were
566 compared between DBH-Cre; Vglut2 cKO cohorts and sibling controls using a linear mixed-effects
567 regression model with animal type (experimental vs. control) as fixed effects and animal ID as a
568 random effect (Lusk et al., 2022). A $p < 0.05$ was used to indicate statistical significance, and
569 individual data points, mean, and standard error of the mean are shown on all charts. The graphs
570 were plotted by Prism 8.
571
572 **Image quantification**
573 Images were taken by using a Zeiss upright epifluorescent microscope and a Zeiss LSM 880 with
574 Airyscan FAST confocal microscope. Images were captured using Zen software with z-stack
575 function from top to bottom with 0.34µm intervals, exported, and then analyzed in Imaris using
576 the spots and surface functions. For quantification of immunofluorescence staining, each GFP

577 positive area coincident with DAPI (to denote nuclear localization) was defined as Vglut2 or
578 Vglut3-expressing NA neurons while each tdTomato positive area coincident with DAPI was
579 defined as NA neurons without any Vglut2 or Vglut3 co-expression. For quantification of Vglut2
580 or Vglut3 with DBH double *in situ* hybridization in adult WT mice, DBH positive areas coinciding
581 with DAPI were identified as NA neurons and the DBH positive areas overlapped with Vglut2/3
582 positive pixels and DAPI were defined as NA neurons colocalized with Vglut2/3. The number of
583 Vglut2/3 positive NA neurons and Vglut2/3 negative NA neurons was counted in each image for
584 both immunofluorescence and in situ experiments and the percentage of Vglut2/3 positive NA
585 neurons among all NA neurons in each NA nucleus in each mouse brainstem was calculated every
586 other brain section unilaterally. For quantification of Vglut2 and DBH double ISH in DBH-Cre;
587 Vglut2 cKO and their littermate controls, Vglut2 pixel intensities in DBH positive areas coincident
588 with DAPI (NA neurons) were measured in mutant and control images separately. The Vglut2
589 pixel intensity in NA neurons of control brains was normalized as 1 and the relative Vglut2 pixel
590 intensity of NA neurons in mutant brains compared to that in control brains was calculated. At
591 least three mouse brains were examined for each set of experiments in each group. All
592 quantitative results were graphed using Prism 8.
593
594 **Data availability**
595 All the data supporting this study is available from the corresponding author upon request.
596
597 **Acknowledgments**
598 We thank the Optical Imaging & Vital Microscopy Core (OiVM) at Baylor College of Medicine with
599 the expert assistance of Jason Kirk for confocal imaging. We thank BCM Neuropathology Core
600 and Tao Lin for tissue sectioning. We thank the RNA In Situ Hybridization Core at Baylor College
601 of Medicine with the expert assistance of Cecilia Ljungberg for performing in situ hybridization
602 (NIH S10 OD016167 and NIH IDDRC Grant P50 HD103555). We thank Dr. Joshua Ortiz and Dr.
603 Benjamin Arenkiel at the NRI Optogenetics and Viral Vectors Core for providing Cre-responsive
604 AAV virus used in viral injection.
605

606 **Author contributions**

607 YC designed and completed immunofluorescence staining, imaging, and plethysmography
608 experiments, analyzed data, wrote the initial manuscript and revised the manuscript.

609 SL completed the viral injection experiments and revised the manuscript.

610 RR conceptualized and designed the study, analyzed the data, and revised the manuscript.

611

612 **Competing interests**

613 No competing interests are declared.

614

615 **Figure 1. Cumulative fate maps of glutamate co-expressing NA neurons characterized by**
616 **intersectional genetics.** (A) Breeding schematic. Vglut1-Cre/+, Vglut2-Cre/+ and Vglut3-Cre/+
617 were each bred with DBH-p2a-Flpo/+ mice respectively. These Vglut1, Vglut2, or Vglut3-Cre/+;
618 DBH-p2a-Flpo/+ compound lines were then crossed with the RC::FLTG intersectional reporter
619 mice. In each of the three intersectional reporter crosses, NA neurons co-expressing either
620 Vglut1, Vglut2, or Vglut3 are labeled by green fluorescent protein (eGFP) while NA neurons
621 without any Vglut1,2, or 3 expression are labelled by red fluorescent protein (tdTomato). Shown
622 as an example is the Vglut2-Cre/+; DBH-p2a-Flpo/+; RC::FLTG/+ intersectional reporter line. (B)
623 Quantification of the percentage of Vglut2-coexpressing NA neurons among NA neurons in each
624 brainstem NA nuclei including A7, LC, A5, sub CD/CV, anterior C1/A1 and C2/A2, posterior C1/A1
625 and C2/A2. (C) Quantification of the percentage of Vglut3-coexpressing NA neurons among NA
626 neurons in each NA nuclei. (D) Fluorescent expression of tdTomato (red) and eGFP (green) in
627 coronal sections of Vglut1, Vglut2, or Vglut3 intersectional reporter lines in brainstem NA nuclei.
628 Nucleus is labeled by DAPI (blue). Scale bar 50µm.

629

630 **Figure 2. Characterization of real time co-expression of Vglut1, Vglut2 and Vglut3 in brainstem**
631 **NA neurons in adult mice by fluorescent *in situ* hybridization.** (A) Representative images of
632 Vglut1, Vglut2, or Vglut3 and DBH double ISH in coronal sections of WT mice in all of brainstem
633 NA nuclei in adult mice. DBH (green), Vglut1/2/3 (red), DAPI (cyan). Scale bar 50µm. (B)

634 Quantification of the percentage of Vglut2 co-expression in NA neurons in each NA nuclei. (C)
635 Quantification of the percentage of Vglut3 co-expression in NA neurons in each NA nuclei.
636
637 **Figure 3. DBH with Vglut2 co-staining by fluorescent *in situ* hybridization confirms that Vglut2**
638 **expression is disrupted in the whole central NA system in DBH-Cre; Vglut2 cKO mice.** (A)
639 Representative images of Vglut2 and DBH double ISH in anterior C1/A1, posterior C1/A1, anterior
640 C2/A2 and posterior C2/A2 in control and DBH-Cre; Vglut2 cKO mice. DBH (green), Vglut2 (red),
641 DAPI (cyan). Scale bar 20µm.(B) Quantification of intensity of Vglut2 signal in control and DBH-
642 Cre; Vglut2 cKO mice.
643
644 **Figure 4. Vglut2 conditional knockout in central noradrenergic neurons fails to alter baseline**
645 **breathing and the hypercapnic ventilatory reflex (5% CO_2).** (A) Mouse model schematic and
646 experimental protocol including habituation and hypercapnia protocol. (B) Under both room air
647 and hypercapnia (5% CO_2), DBH-Cre; Vglut2 cKO mice didn't show significant changes in
648 respiratory output (V_E/V_{O2}), minute ventilation (V_E), respiratory rate (V_f), tidal volume (V_T), and
649 metabolism demand (V_{O2}). Linear mixed-effects regression model, *p<0.05.
650
651 **Figure 5. Vglut2 conditional knockout in central noradrenergic neurons fails to alter the**
652 **majority of hypercapnic ventilation parameters and metabolism under 7% CO_2.** (A) Mouse
653 model schematic and experimental protocol including habituation and hypercapnia protocol. (B)
654 Knocking out Vglut2 in the whole NA system failed to alter ventilation (V_E/V_{O2}, V_f, V_E) and
655 metabolism (V_{O2}) but only showed a significantly reduce in V_T under 7% CO_2 condition. Linear
656 mixed-effects regression model, *p<0.05.
657
658 **Figure 6. Vglut2 conditional knockout in central noradrenergic neurons fails to alter the**
659 **hypercapnic ventilatory reflex (10% CO_2).** (A) Mouse model schematic and experimental
660 protocol including habituation and hypercapnia protocol. (B) Knocking out Vglut2 in the whole
661 NA system didn't significantly alter ventilation (V_E/V_{O2}, V_f, V_T, V_E) and metabolism (V_{O2}) under 10%
662 CO_2 condition. Linear mixed-effects regression model, *p<0.05.

663 **Figure 7. Vglut2 conditional knockout in central noradrenergic neurons fails to alter the hypoxic**
664 **ventilatory reflex (10% O_2).** (A) Mouse model schematic and experimental protocol including
665 habituation and hypoxia protocol. (B) Knocking out Vglut2 in the whole NA system didn't show
666 significant breathing changes including V_E/V_{O2}, V_E, V_f, V_T, and V_{O2} in either of the three five-minute
667 time periods under hypoxia (10% O_2). Linear mixed-effects regression model, *p<0.05.
668
669 **Figure 2 Supplement 1. Virus injection of Cre-dependent tdTomato into LC of Vglut2-Cre mice.**

670 **Table 1.** Respiratory and metabolic values under room air conditions and the statistical tests.

671 **Table 2.** Respiratory and metabolic values under 5% CO_2 conditions and the statistical tests.

672 **Table 3.** Respiratory and metabolic values under 7% CO_2 conditions and the statistical tests.

673 **Table 4.** Respiratory and metabolic values under 10% CO_2 conditions and the statistical tests.

674 **Table 5.** Respiratory and metabolic values under 10% O_2 conditions and the statistical tests.

675 **Supplemental table 1.** Vglut2 positive innervations from central noradrenergic neurons to the
676 brain nuclei important in breathing control.

677
678 **References**
679

680 Abbott SBG, DePuy SD, Nguyen T, Coates MB, Stornetta RL, Guyenet PG. 2013. Selective
681 optogenetic activation of rostral ventrolateral medullary catecholaminergic neurons
682 produces cardiorespiratory stimulation in conscious mice. *J Neurosci* **33**:3164–3177.
683 doi:10.1523/JNEUROSCI.1046-12.2013
684 Abbott SBG, Holloway BB, Viar KE, Guyenet PG. 2014. Vesicular glutamate transporter 2 is
685 required for the respiratory and parasympathetic activation produced by optogenetic
686 stimulation of catecholaminergic neurons in the rostral ventrolateral medulla of mice in vivo.
687 *Eur J Neurosci* **39**:98–106. doi:10.1111/ejn.12421
688 Beltrán-Castillo S, Olivares MJ, Contreras RA, Zúñiga G, Llona I, von Bernhardi R, Eugenín JL.
689 2017. D-serine released by astrocytes in brainstem regulates breathing response to CO2
690 levels. *Nat Commun* **8**:838. doi:10.1038/s41467-017-00960-3
691 Chigr F, Najimi M, Jordan D, Denoroy L, Pearson J, Tommasi M, Gilly R, Kopp N. 1989.
692 [Immunohistochemical absence of adrenergic neurons in the dorsal part of the solitary tract
693 nucleus in sudden infant death]. *C R Acad Sci III, Sci Vie* **309**:543–549.
694 Comer AM, Qi J, Christie DL, Gibbons HM, Lipski J. 1998. Noradrenaline transporter expression
695 in the pons and medulla oblongata of the rat: localisation to noradrenergic and some C1
696 adrenergic neurones. *Brain Res Mol Brain Res* **62**:65–76. doi:10.1016/s0169-328x(98)00241-1

697 Del Negro CA, Funk GD, Feldman JL. 2018. Breathing matters. *Nat Rev Neurosci* **19**:351–367.
698 doi:10.1038/s41583-018-0003-6
699 DePuy SD, Stornetta RL, Bochorishvili G, Deisseroth K, Witten I, Coates M, Guyenet PG. 2013.
700 Glutamatergic neurotransmission between the C1 neurons and the parasympathetic
701 preganglionic neurons of the dorsal motor nucleus of the vagus. *J Neurosci* **33**:1486–1497.
702 doi:10.1523/JNEUROSCI.4269-12.2013
703 Dick TE, Dutschmann M, Feldman JL, Fong AY, Hülsmann S, Morris KM, Ramirez JM, Smith JC,
704 Respiratory Neurobiology Consortium. 2018. Facts and challenges in respiratory
705 neurobiology. *Respir Physiol Neurobiol* **258**:104–107. doi:10.1016/j.resp.2015.01.014
706 Ducros L, Vahedi K, Similowski T, Bousser M-G, Payen D. 2003. Uncontrollable high-frequency
707 tachypnea in a case of unilateral medial medullary infarct. *Intensive Care Med* **29**:841–844.
708 doi:10.1007/s00134-003-1658-6
709 Feldman JL, Del Negro CA, Gray PA. 2013. Understanding the rhythm of breathing: so near, yet
710 so far. *Annu Rev Physiol* **75**:423–452. doi:10.1146/annurev-physiol-040510-130049
711 Fremeau RT, Voglmaier S, Seal RP, Edwards RH. 2004. VGLUTs define subsets of excitatory
712 neurons and suggest novel roles for glutamate. *Trends Neurosci* **27**:98–103.
713 doi:10.1016/j.tins.2003.11.005
714 Garcia AJ, Koschnitzky JE, Ramirez J-M. 2013. The physiological determinants of sudden infant
715 death syndrome. *Respir Physiol Neurobiol* **189**:288–300. doi:10.1016/j.resp.2013.05.032
716 Gauda EB, Cristofalo E, Nunez J. 2007. Peripheral arterial chemoreceptors and sudden infant
717 death syndrome. *Respir Physiol Neurobiol* **157**:162–170. doi:10.1016/j.resp.2007.02.016
718 Guyenet PG, Stornetta RL, Bochorishvili G, Depuy SD, Burke PGR, Abbott SBG. 2013. C1
719 neurons: the body's EMTs. *Am J Physiol Regul Integr Comp Physiol* **305**:R187-204.
720 doi:10.1152/ajpregu.00054.2013
721 Haxhiu MA, Yung K, Erokwu B, Cherniack NS. 1996. CO2-induced c-fos expression in the CNS
722 catecholaminergic neurons. *Respir Physiol* **105**:35–45. doi:10.1016/0034-5687(96)00034-5
723 Henneberger C, Bard L, Panatier A, Reynolds JP, Kopach O, Medvedev NI, Minge D, Herde MK,
724 Anders S, Kraev I, Heller JP, Rama S, Zheng K, Jensen TP, Sanchez-Romero I, Jackson CJ,
725 Janovjak H, Ottersen OP, Nagelhus EA, Oliet SHR, Stewart MG, Nägerl UV, Rusakov DA. 2020.
726 LTP induction boosts glutamate spillover by driving withdrawal of perisynaptic astroglia.
727 *Neuron* **108**:919-936.e11. doi:10.1016/j.neuron.2020.08.030
728 Hülsmann S, Oku Y, Zhang W, Richter DW. 2000. Metabotropic glutamate receptors and
729 blockade of glial Krebs cycle depress glycinergic synaptic currents of mouse hypoglossal
730 motoneurons. *Eur J Neurosci* **12**:239–246.
731 Kopp N, Chigr F, Denoroy L, Gilly R, Jordan D. 1993. Absence of adrenergic neurons in nucleus
732 tractus solitarius in sudden infant death syndrome. *Neuropediatrics* **24**:25–29. doi:10.1055/s-
733 2008-1071508
734 Lorang D, Amara SG, Simerly RB. 1994. Cell-type-specific expression of catecholamine
735 transporters in the rat brain. *J Neurosci* **14**:4903–4914. doi:10.1523/JNEUROSCI.14-08-
736 04903.1994
737 Lusk S, Ward CS, Chang A, Twitchell-Heyne A, Fattig S, Allen G, Jankowsky J, Ray R. 2022.
738 Breathe Easy, an automated respiratory data pipeline for waveform characteristic analysis.
739 *BioRxiv*. doi:10.1101/2022.12.02.518741

740 Malheiros-Lima MR, Silva JN, Souza FC, Takakura AC, Moreira TS. 2020. C1 neurons are part of
741 the circuitry that recruits active expiration in response to the activation of peripheral
742 chemoreceptors. *eLife* **9**. doi:10.7554/eLife.52572
743 Malheiros-Lima MR, Silva TM, Takakura AC, Moreira TS. 2022. A5 noradrenergic-projecting C1
744 neurons activate sympathetic and breathing outputs in anaesthetized rats. *Exp Physiol*
745 **107**:147–160. doi:10.1113/EP089691
746 Malheiros-Lima MR, Totola LT, Lana MVG, Strauss BE, Takakura AC, Moreira TS. 2018. Breathing
747 responses produced by optogenetic stimulation of adrenergic C1 neurons are dependent on
748 the connection with preBötzinger complex in rats. *Pflugers Arch* **470**:1659–1672.
749 doi:10.1007/s00424-018-2186-0
750 Mansouri J, Panigrahy A, Filiano JJ, Sleeper LA, St John WM, Kinney HC. 2001. Alpha2 receptor
751 binding in the medulla oblongata in the sudden infant death syndrome. *J Neuropathol Exp*
752 *Neurol* **60**:141–146.
753 Martinez VK, Saldana-Morales F, Sun JJ, Zhu PJ, Costa-Mattioli M, Ray RS. 2019. Off-Target
754 Effects of Clozapine-N-Oxide on the Chemosensory Reflex Are Masked by High Stress Levels.
755 *Front Physiol* **10**:521. doi:10.3389/fphys.2019.00521
756 Ozawa Y, Takashima S, Tada H. 2003. Alpha2-adrenergic receptor subtype alterations in the
757 brainstem in the sudden infant death syndrome. *Early Hum Dev* **75 Suppl**:S129-38.
758 doi:10.1016/j.earlhumdev.2003.08.016
759 Ramirez J-M, Karlen-Amarante M, Wang J-DJ, Bush NE, Carroll MS, Weese-Mayer DE, Huff A.
760 2020. The pathophysiology of rett syndrome with a focus on breathing dysfunctions.
761 *Physiology (Bethesda)* **35**:375–390. doi:10.1152/physiol.00008.2020
762 Ray RS, Corcoran AE, Brust RD, Kim JC, Richerson GB, Nattie E, Dymecki SM. 2011. Impaired
763 respiratory and body temperature control upon acute serotonergic neuron inhibition. *Science*
764 **333**:637–642. doi:10.1126/science.1205295
765 Roux J-C, Dura E, Moncla A, Mancini J, Villard L. 2007. Treatment with desipramine improves
766 breathing and survival in a mouse model for Rett syndrome. *Eur J Neurosci* **25**:1915–1922.
767 doi:10.1111/j.1460-9568.2007.05466.x
768 Souza GMPR, Stornetta DS, Vitali AJ, Wildner H, Zeilhofer HU, Campbell JN, Abbott SBG. 2022a.
769 Chemogenetic activation of noradrenergic A5 neurons increases blood pressure and visceral
770 sympathetic activity in adult rats. *Am J Physiol Regul Integr Comp Physiol* **323**:R512–R531.
771 doi:10.1152/ajpregu.00119.2022
772 Souza GMPR, Stornetta RL, Stornetta DS, Guyenet PG, Abbott SBG. 2022b. Adrenergic C1
773 neurons monitor arterial blood pressure and determine the sympathetic response to
774 hemorrhage. *Cell Rep* **38**:110480. doi:10.1016/j.celrep.2022.110480
775 Stornetta RL, Sevigny CP, Guyenet PG. 2002a. Vesicular glutamate transporter DNPI/VGLUT2
776 mRNA is present in C1 and several other groups of brainstem catecholaminergic neurons. *J*
777 *Comp Neurol* **444**:191–206. doi:10.1002/cne.10141
778 Stornetta RL, Sevigny CP, Schreihofer AM, Rosin DL, Guyenet PG. 2002b. Vesicular glutamate
779 transporter DNPI/VGLUT2 is expressed by both C1 adrenergic and nonaminergic
780 presympathetic vasomotor neurons of the rat medulla. *J Comp Neurol* **444**:207–220.
781 doi:10.1002/cne.10142

782 Stubbusch J, Majdazari A, Schmidt M, Schütz G, Deller T, Rohrer H. 2011. Generation of the
783 tamoxifen-inducible DBH-Cre transgenic mouse line DBH-CT. *Genesis* **49**:935–941.
784 doi:10.1002/dvg.20773
785 Sun JJ, Ray R. 2016. Generation of Two Noradrenergic-Specific Dopamine-Beta-Hydroxylase-
786 FLPo Knock-In Mice Using CRISPR/Cas9-Mediated Targeting in Embryonic Stem Cells. *PLoS*
787 *ONE* **11**:e0159474. doi:10.1371/journal.pone.0159474
788 Takashima S, Becker LE. 1991. Delayed dendritic development of catecholaminergic neurons in
789 the ventrolateral medulla of children who died of sudden infant death syndrome.
790 *Neuropediatrics* **22**:97–99. doi:10.1055/s-2008-1071424
791 Tong Q, Ye C, McCrimmon RJ, Dhillon H, Choi B, Kramer MD, Yu J, Yang Z, Christiansen LM, Lee
792 CE, Choi CS, Zigman JM, Shulman GI, Sherwin RS, Elmquist JK, Lowell BB. 2007. Synaptic
793 glutamate release by ventromedial hypothalamic neurons is part of the neurocircuitry that
794 prevents hypoglycemia. *Cell Metab* **5**:383–393. doi:10.1016/j.cmet.2007.04.001
795 Viemari J-C, Roux J-C, Tryba AK, Saywell V, Burnet H, Peña F, Zanella S, Bévengut M,
796 Barthelemy-Requin M, Herzing LBK, Moncla A, Mancini J, Ramirez J-M, Villard L, Hilaire G.
797 2005. Mecp2 deficiency disrupts norepinephrine and respiratory systems in mice. *J Neurosci*
798 **25**:11521–11530. doi:10.1523/JNEUROSCI.4373-05.2005
799 Viemari J-C. 2008. Noradrenergic modulation of the respiratory neural network. *Respir Physiol*
800 *Neurobiol* **164**:123–130. doi:10.1016/j.resp.2008.06.016
801 Yang B, Sanches-Padilla J, Kondapalli J, Morison SL, Delpire E, Awatramani R, Surmeier DJ. 2021.
802 Locus coeruleus anchors a trisynaptic circuit controlling fear-induced suppression of feeding.
803 *Neuron* **109**:823-838.e6. doi:10.1016/j.neuron.2020.12.023
804 Yang CF, Feldman JL. 2018. Efferent projections of excitatory and inhibitory preBötzinger
805 Complex neurons. *J Comp Neurol* **526**:1389–1402. doi:10.1002/cne.24415
806 Yaylaoglu MB, Titmus A, Visel A, Alvarez-Bolado G, Thaller C, Eichele G. 2005. Comprehensive
807 expression atlas of fibroblast growth factors and their receptors generated by a novel robotic
808 in situ hybridization platform. *Dev Dyn* **234**:371–386. doi:10.1002/dvdy.20441

Figure 1

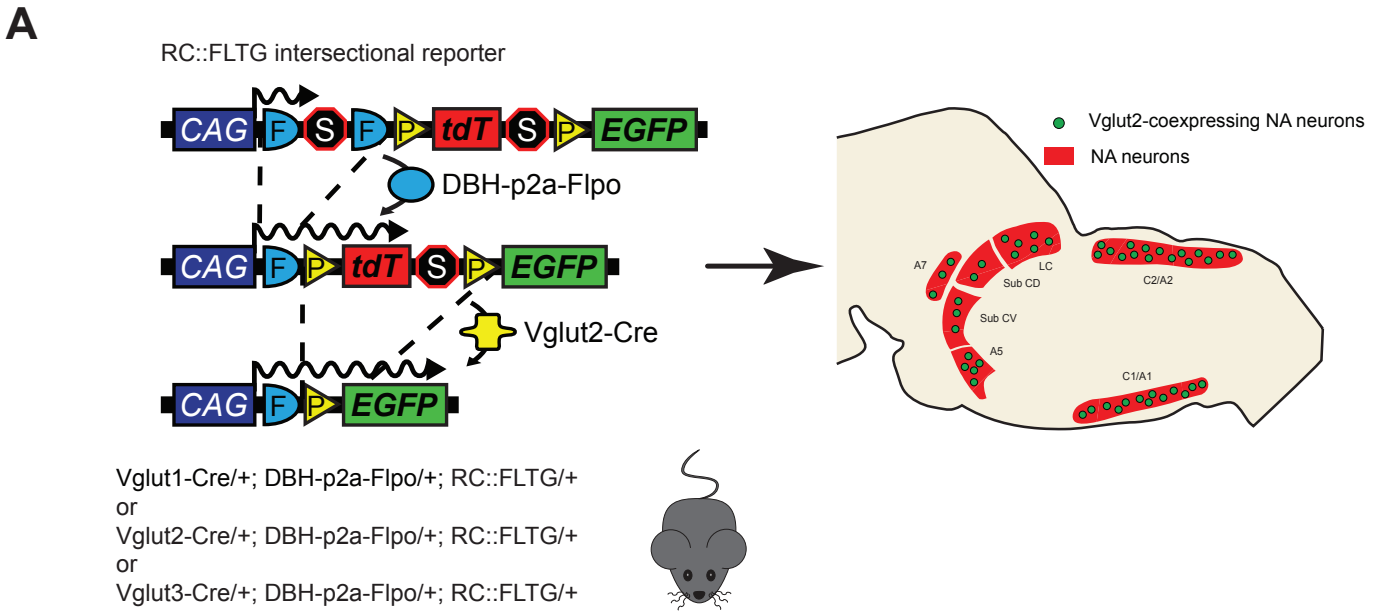
A
RC::FLTG intersectional reporter
CAG
F
S
F
P
tdT
S
P
EGFP
DBH-p2a-Flpo
CAG
F
P
tdT
S
P
EGFP
Vglut2-Cre
CAG
F
P
EGFP
Vglut2-coexpressing NA neurons
NA neurons
A7
LC
Sub CD
C2/A2
Sub CV
A5
C1/A1
Vglut1-Cre/+; DBH-p2a-Flpo/+; RC::FLTG/+
or
Vglut2-Cre/+; DBH-p2a-Flpo/+; RC::FLTG/+
or
Vglut3-Cre/+; DBH-p2a-Flpo/+; RC::FLTG/+

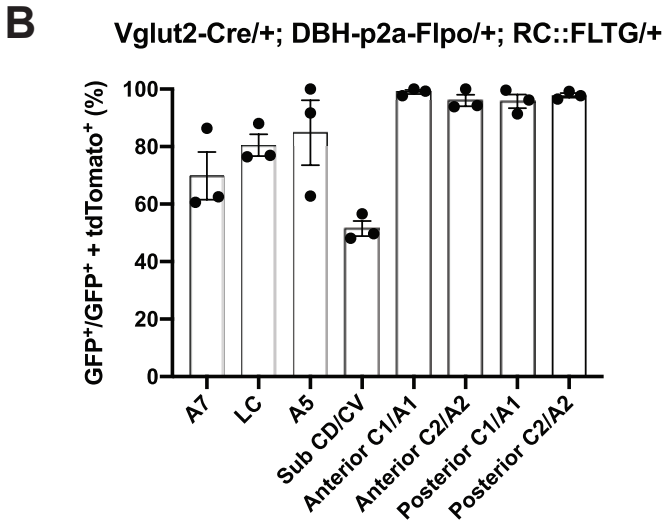
B
Vglut2-Cre/+; DBH-p2a-Flpo/+; RC::FLTG/+
GFP+/GFP+ + tdTomato+ (%)
100
80
60
40
20
0
A7
LC
A5
Sub CD/CV
Anterior C1/A1
Anterior C2/A2
Posterior C1/A1
Posterior C2/A2

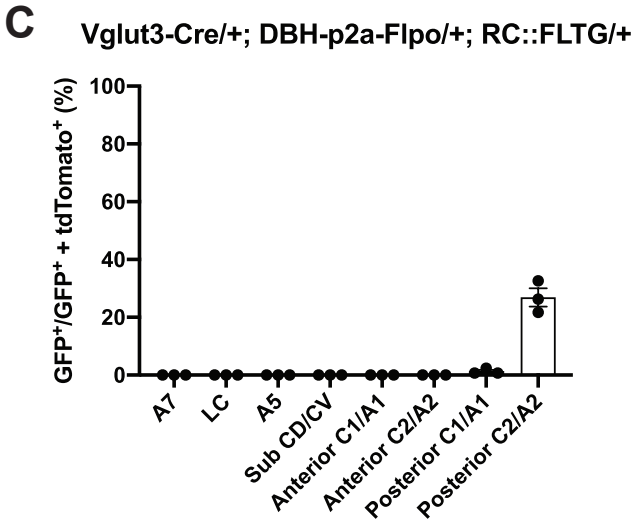
C
Vglut3-Cre/+; DBH-p2a-Flpo/+; RC::FLTG/+
GFP+/GFP+ + tdTomato+ (%)
100
80
60
40
20
0
A7
LC
A5
Sub CD/CV
Anterior C1/A1
Anterior C2/A2
Posterior C1/A1
Posterior C2/A2

Figure 1. cont.

D

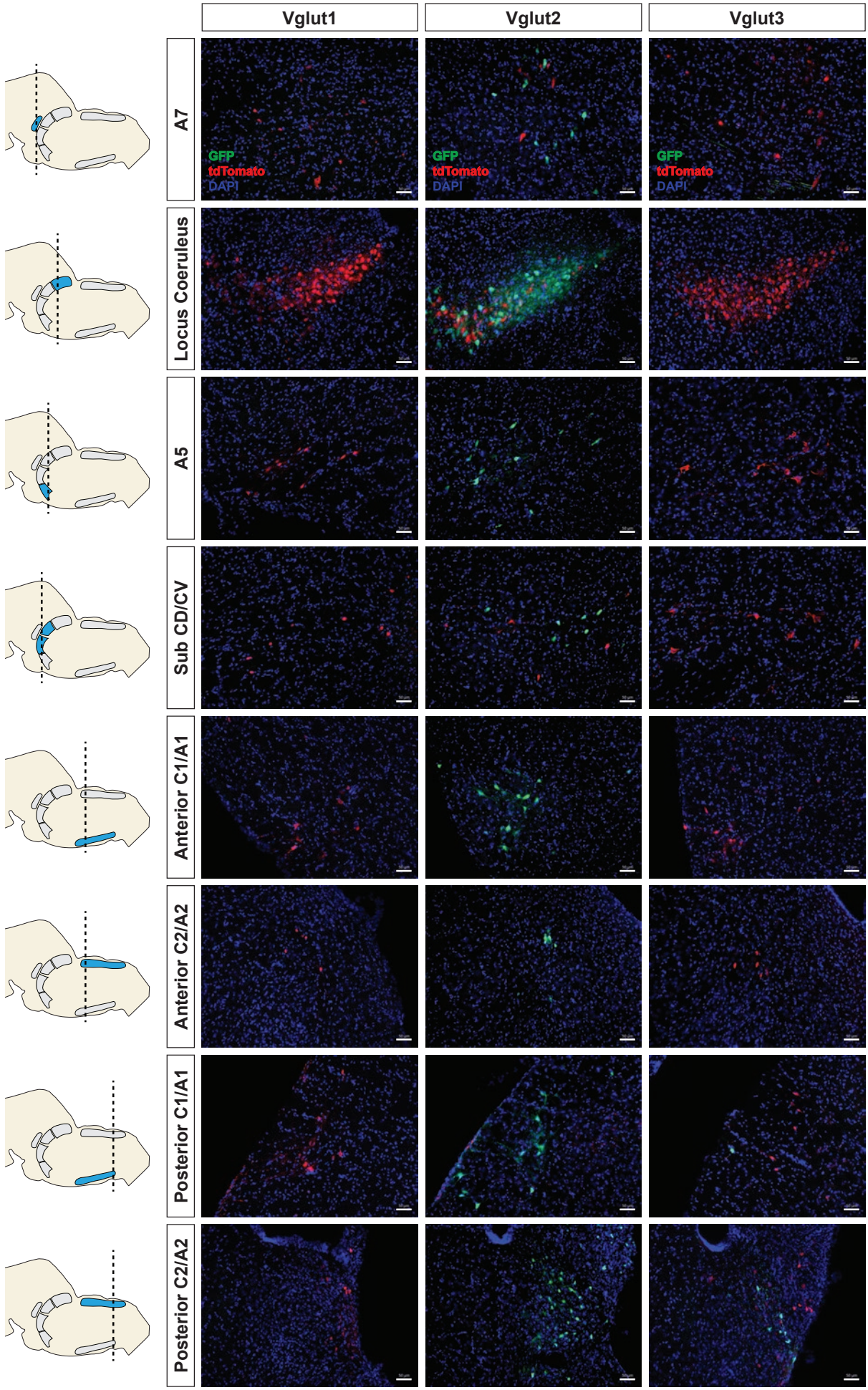

Figure 2

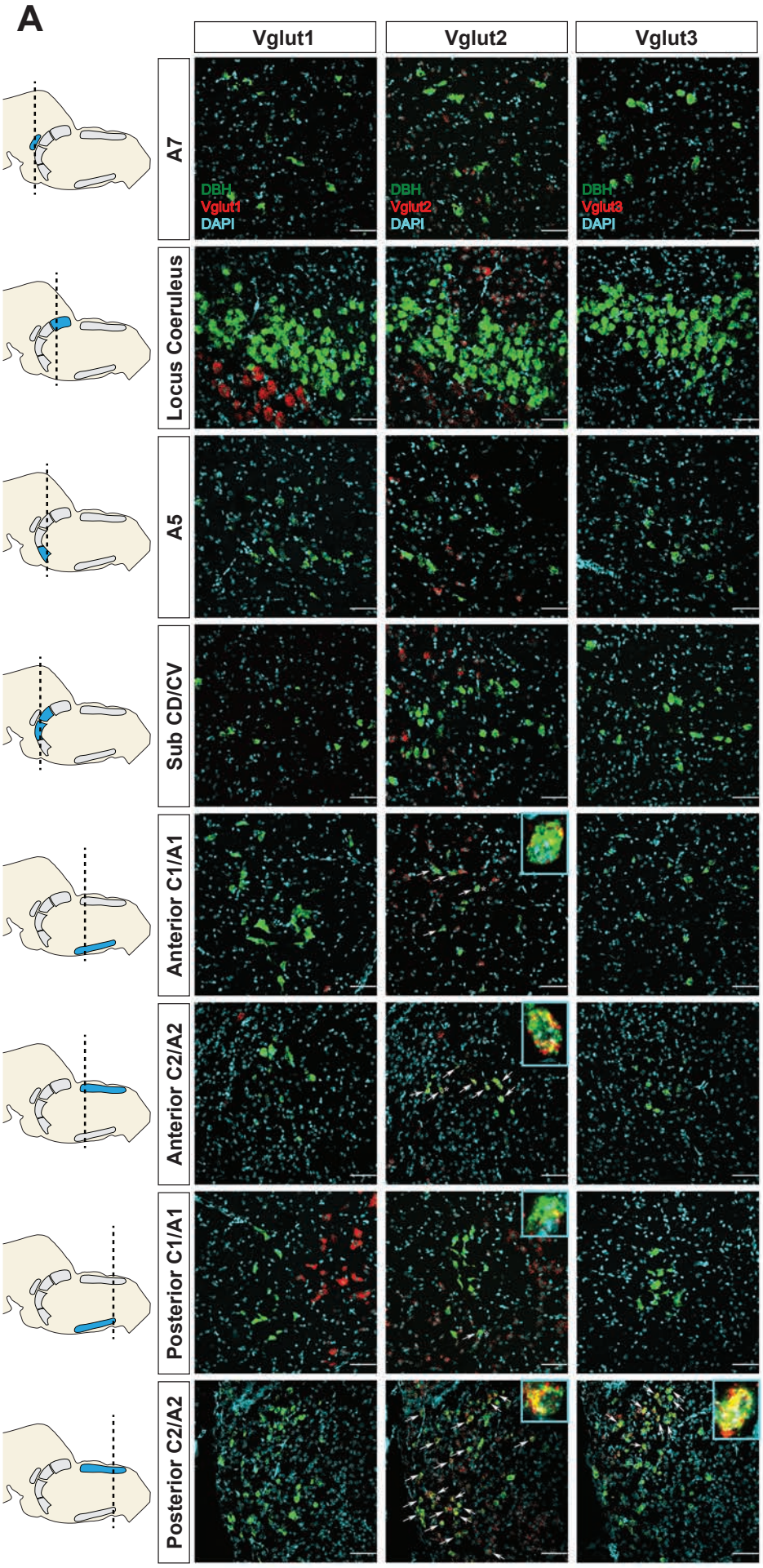
A
Vglut1
Vglut2
Vglut3
A7
Locus Coeruleus
A5
Sub CD/CV
Anterior C1/A1
Anterior C2/A2
Posterior C1/A1
Posterior C2/A2
DBH
Vglut1
DAPI
DBH
Vglut2
DAPI
DBH
Vglut3
DAPI

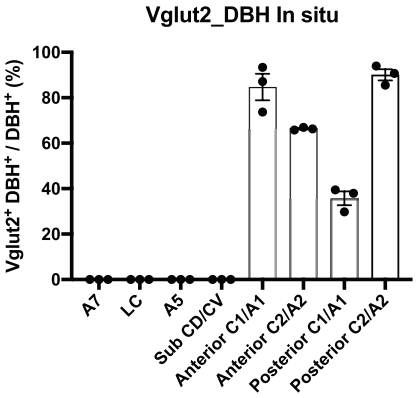
B
Vglut2_DBH In situ
Vglut2+ DBH+ / DBH+ (%)
100
80
60
40
20
0
A7
LC
A5
Sub CD/CV
Anterior C1/A1
Anterior C2/A2
Posterior C1/A1
Posterior C2/A2

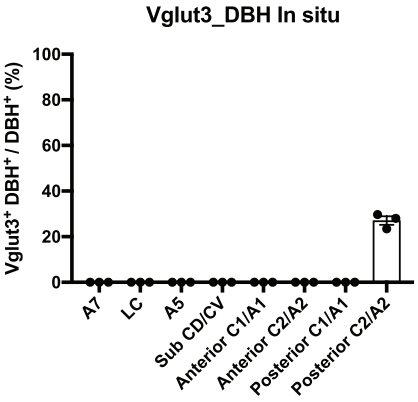
C
Vglut3_DBH In situ
Vglut3+ DBH+ / DBH+ (%)
100
80
60
40
20
0
A7
LC
A5
Sub CD/CV
Anterior C1/A1
Anterior C2/A2
Posterior C1/A1
Posterior C2/A2

Figure 3

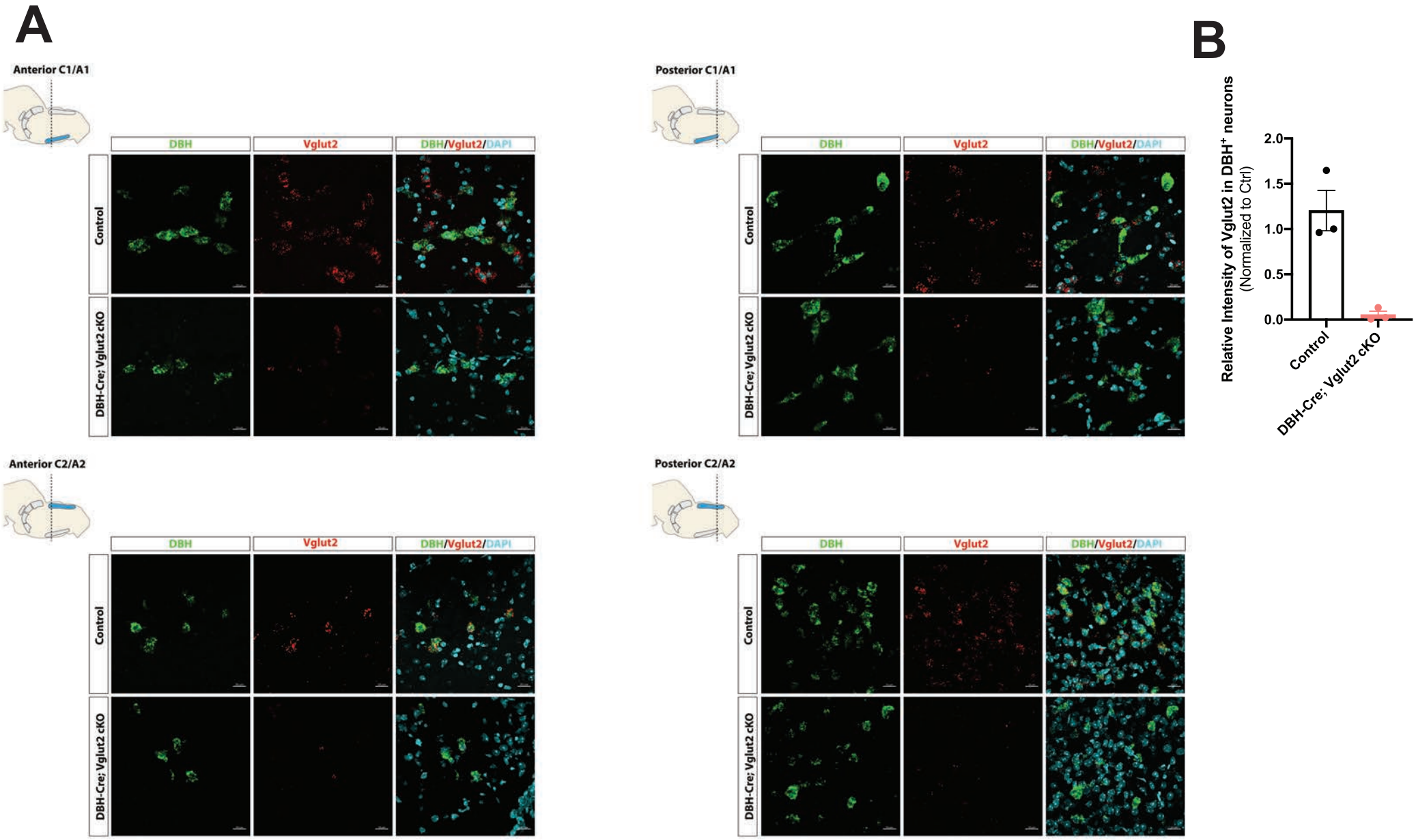
A
Anterior C1/A1
Posterior C1/A1
Anterior C2/A2
Posterior C2/A2
DBH
Vglut2
DBH/Vglut2/DAPI
Control
DBH-Cre; Vglut2 cKO
B
Relative Intensity of Vglut2 in DBH+ neurons
(Normalized to Ctrl)
2.0
1.5
1.0
0.5
0.0
Control
DBH-Cre; Vglut2 cKO

Figure 4

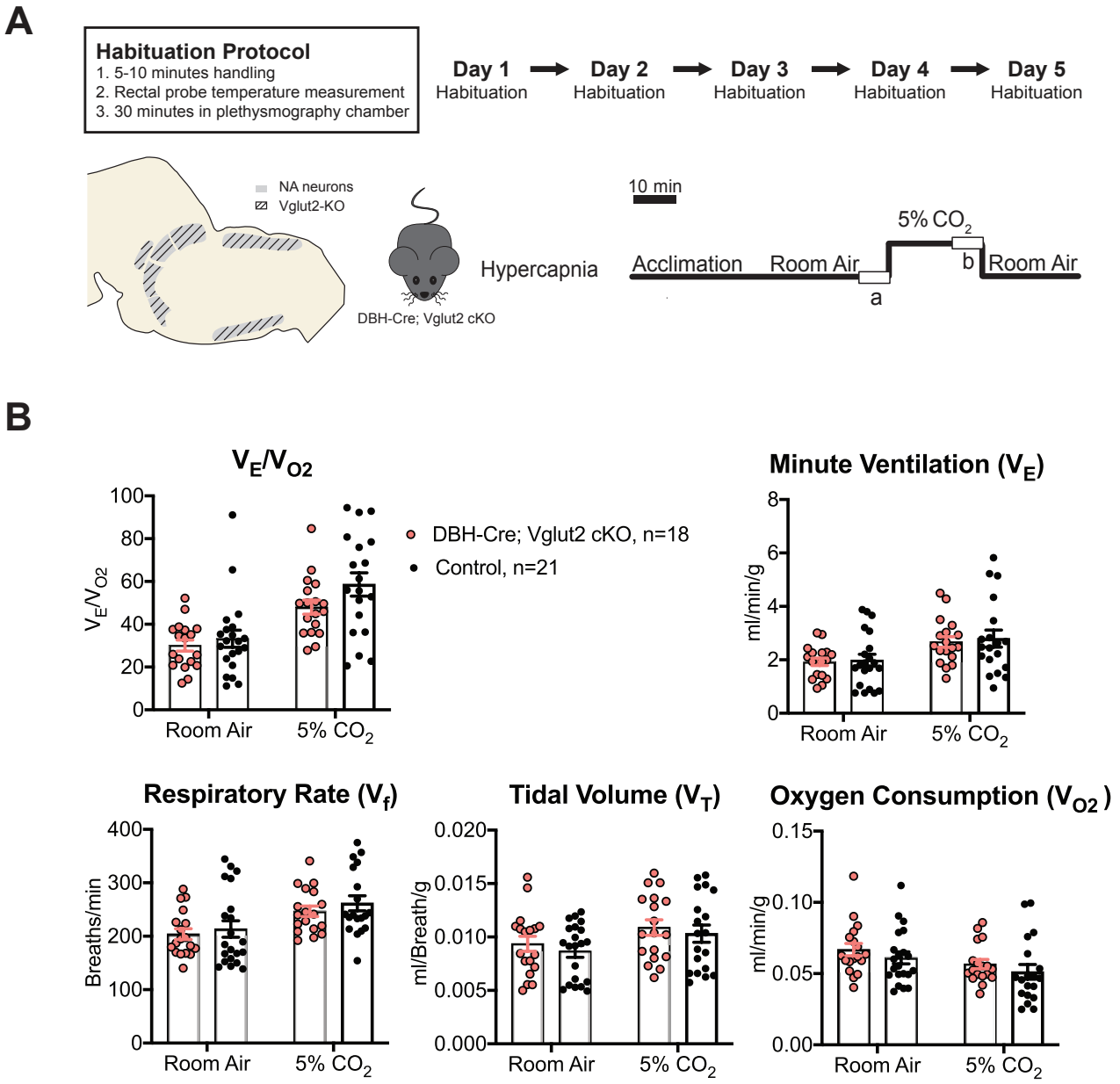
A
Habituation Protocol
1. 5-10 minutes handling
2. Rectal probe temperature measurement
3. 30 minutes in plethysmography chamber
Day 1 Habituation
Day 2 Habituation
Day 3 Habituation
Day 4 Habituation
Day 5 Habituation
NA neurons
Vglut2-KO
DBH-Cre; Vglut2 cKO
Hypercapnia
10 min
Acclimation
Room Air
5% CO2
a
b
Room Air
B
VE/VO2
DBH-Cre; Vglut2 cKO, n=18
Control, n=21
Minute Ventilation (VE)
ml/min/g
Respiratory Rate (Vf)
Breaths/min
Tidal Volume (VT)
ml/Breath/g
Oxygen Consumption (VO2)
ml/min/g
Room Air
5% CO2

Figure 5

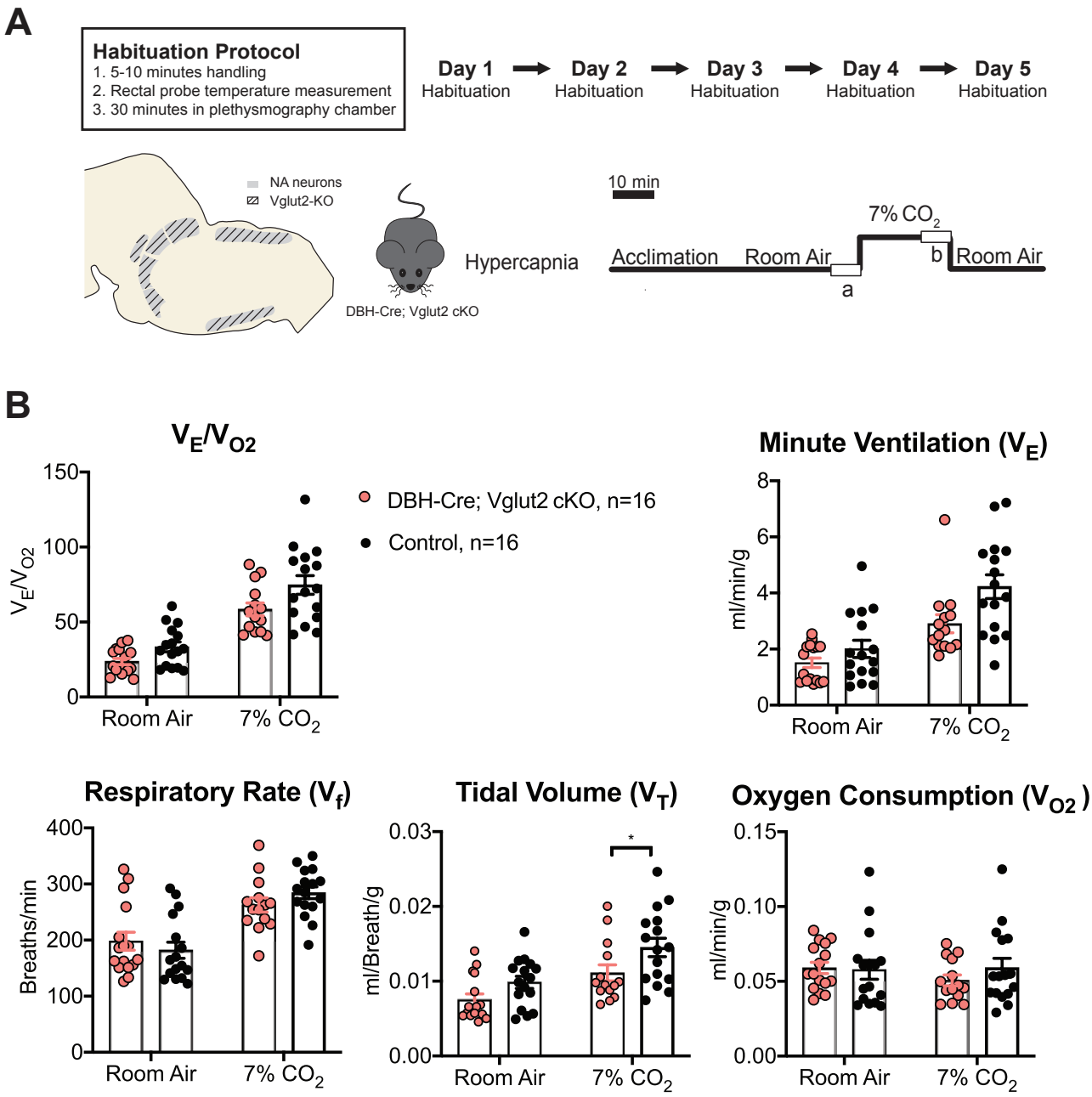
A
Habituation Protocol
1. 5-10 minutes handling
2. Rectal probe temperature measurement
3. 30 minutes in plethysmography chamber
Day 1 Habituation
Day 2 Habituation
Day 3 Habituation
Day 4 Habituation
Day 5 Habituation
NA neurons
Vglut2-KO
DBH-Cre; Vglut2 cKO
Hypercapnia
10 min
Acclimation
Room Air
7% CO2
a
b
Room Air
B
VE/VO2
DBH-Cre; Vglut2 cKO, n=16
Control, n=16
Room Air
7% CO2
Minute Ventilation (VE)
ml/min/g
Respiratory Rate (Vf)
Breaths/min
Tidal Volume (VT)
ml/Breath/g
*
Oxygen Consumption (VO2)
ml/min/g

Figure 6

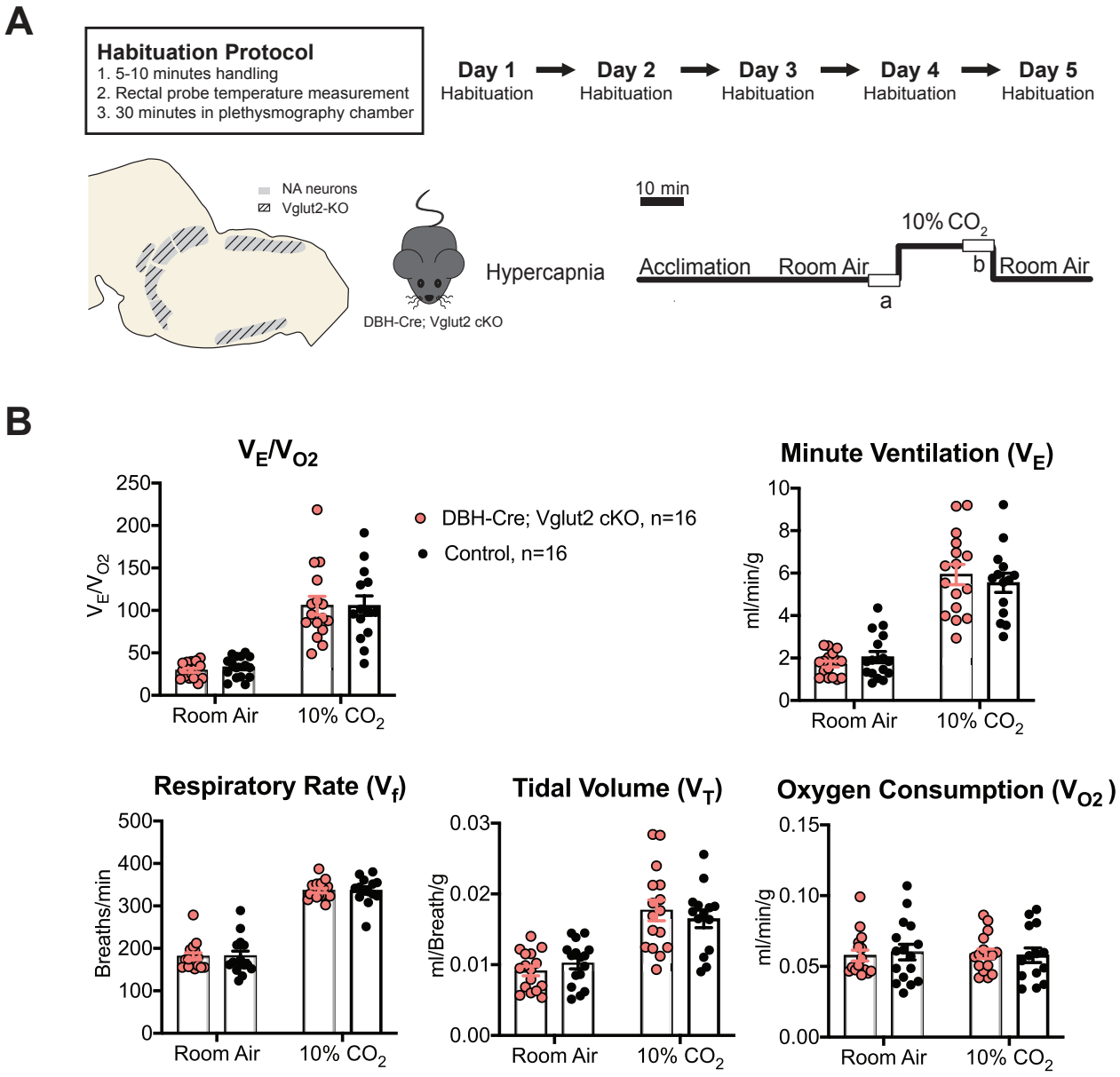
A
Habituation Protocol
1. 5-10 minutes handling
2. Rectal probe temperature measurement
3. 30 minutes in plethysmography chamber
Day 1 Habituation
Day 2 Habituation
Day 3 Habituation
Day 4 Habituation
Day 5 Habituation
NA neurons
Vglut2-KO
DBH-Cre; Vglut2 cKO
Hypercapnia
10 min
Acclimation
Room Air
10% CO2
a
b
Room Air
B
VE/VO2
DBH-Cre; Vglut2 cKO, n=16
Control, n=16
Minute Ventilation (VE)
ml/min/g
Respiratory Rate (Vf)
Breaths/min
Tidal Volume (VT)
ml/Breath/g
Oxygen Consumption (VO2)
ml/min/g
Room Air
10% CO2

Figure 7

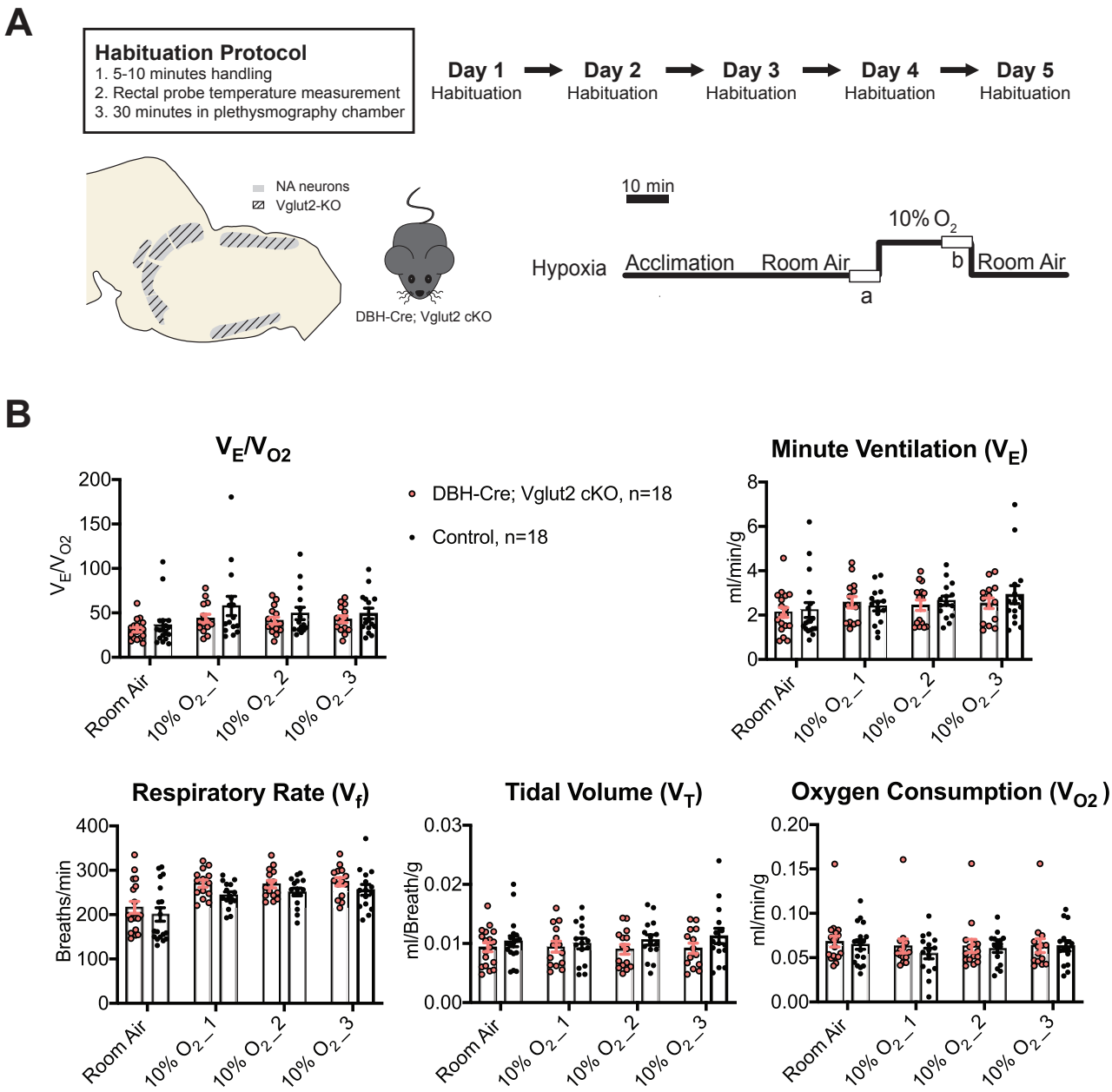
A
Habituation Protocol
1. 5-10 minutes handling
2. Rectal probe temperature measurement
3. 30 minutes in plethysmography chamber
Day 1 Habituation
Day 2 Habituation
Day 3 Habituation
Day 4 Habituation
Day 5 Habituation
NA neurons
Vglut2-KO
DBH-Cre; Vglut2 cKO
10 min
Hypoxia
Acclimation
Room Air
10% O2
a
b
Room Air
B
VE/VO2
DBH-Cre; Vglut2 cKO, n=18
Control, n=18
Minute Ventilation (VE)
ml/min/g
Respiratory Rate (Vf)
Breaths/min
Tidal Volume (VT)
ml/Breath/g
Oxygen Consumption (VO2)
Room Air
10% O2_1
10% O2_2
10% O2_3

Figure 2 supplement 1

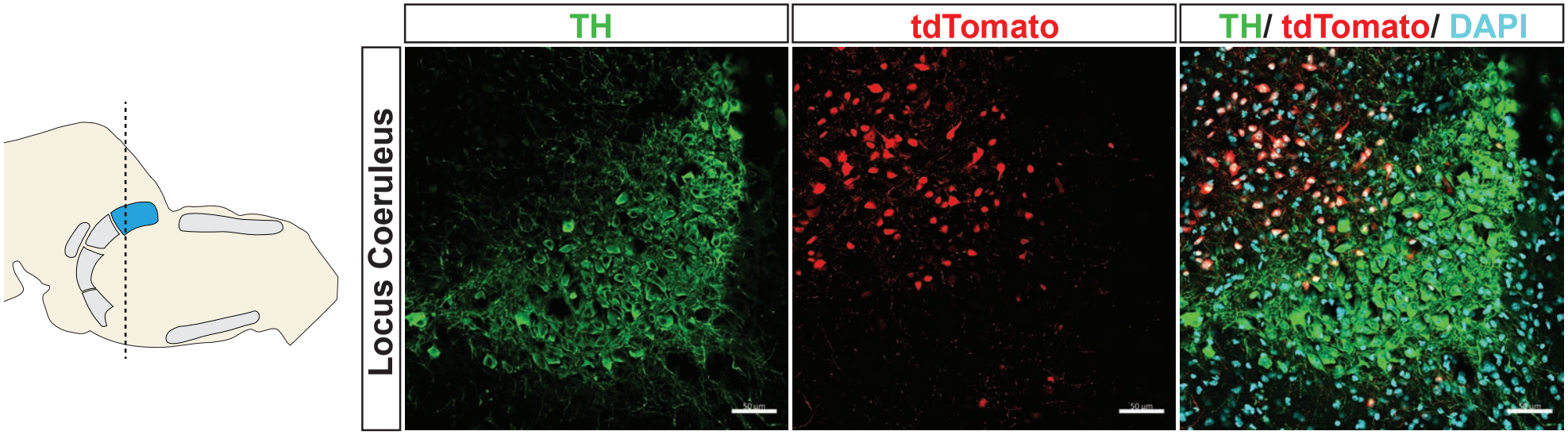

Table 1. Respiratory and metabolic values under room air conditions and the statistical tests

	DBH-Cre; Vglut2 cKO Mean ± SEM	Control Mean ± SEM	DBH-Cre; Vglut2 cKO vs Control linear mixed-effects regression model
V_E/V_{O2}	30.01 ± 2.58	33.22 ± 3.97	P = 0.98
V_f	204.08 ± 10.04	213.58 ± 15.36	P = 0.98
V_T	0.009 ± 0.0007	0.009 ± 0.0006	P = 0.88
V_E	1.93 ± 0.14	1.98 ± 0.22	P = 0.995
V_{O2}	0.067 ± 0.004	0.061 ± 0.004	P = 0.78

Table 2. Respiratory and metabolic values under 5% CO_2 conditions and the statistical tests

	DBH-Cre; Vglut2 cKO Mean ± SEM	Control Mean ± SEM	DBH-Cre; Vglut2 cKO vs Control linear mixed-effects regression model
V_E/V_{O2}	47.99 ± 3.28	58.60 ± 5.44	P = 0.33
V_f	246.72 ± 9.78	261.66 ± 14.00	P = 0.24
V_T	0.011 ± 0.0007	0.010 ± 0.0008	P = 0.81
V_E	2.67 ± 0.20	2.80 ± 0.32	P = 0.98
V_{O2}	0.057 ± 0.003	0.051 ± 0.005	P = 0.42

Table 3. Respiratory and metabolic values under 7% CO_2 conditions and the statistical tests

	DBH-Cre; Vglut2 cKO Mean ± SEM	Control Mean ± SEM	DBH-Cre; Vglut2 cKO vs Control linear mixed-effects regression model
V_E/V_{O2}	58.48 ± 4.29	74.70 ± 6.22	P = 0.23
V_f	262.69 ± 12.82	284.44 ± 10.59	P = 0.98
V_T	0.011 ± 0.0011	0.015 ± 0.0012	P = 0.023*
V_E	2.90 ± 0.32	4.23 ± 0.43	P = 0.16
V_{O2}	0.051 ± 0.004	0.059 ± 0.006	P = 0.64

Table 4. Respiratory and metabolic values under 10% CO_2 conditions and the statistical tests

	DBH-Cre; Vglut2 cKO Mean ± SEM	Control Mean ± SEM	DBH-Cre; Vglut2 cKO vs Control linear mixed-effects regression model
V_E/V_{O2}	105.77 ± 10.80	105.69 ± 11.51	P = 0.9996
V_f	336.31 ± 5.26	336.38 ± 8.52	P = 0.9997
V_T	0.018 ± 0.0015	0.016 ± 0.0012	P = 0.98
V_E	5.94 ± 0.48	5.54 ± 0.45	P = 0.9996
V_{O2}	0.059 ± 0.003	0.058 ± 0.005	P = 0.9999999

Table 5. Respiratory and metabolic values under 10% O_2 conditions and the statistical tests

	DBH-Cre; Vglut2 cKO Mean ± SEM	Control Mean ± SEM	Linear mixed-effects regression model	DBH-Cre; Vglut2 cKO Mean ± SEM	Control Mean ± SEM	Linear mixed-effects regression model	DBH-Cre; Vglut2 cKO Mean ± SEM	Control Mean ± SEM	Linear mixed-effects regression model
	10% O_2_1			10% O_2_2			10% O_2_3		
V_E/V_{O2}	43.79 ± 4.57	57.75 ± 10.88	P = 0.99	41.30 ± 3.85	49.36 ± 6.93	P = 0.99	42.82 ± 3.97	49.19 ± 6.02	P = 0.99
V_f	269.71 ± 8.49	243.89 ± 7.64	P = 0.67	268.38 ± 8.40	251.15 ± 8.67	P = 0.83	273.96 ± 9.31	255.84 ± 12.19	P = 0.80
V_T	0.009 ± 0.0009	0.010 ± 0.0009	P = 0.89	0.009 ± 0.0008	0.011 ± 0.0009	P = 0.85	0.009 ± 0.0009	0.011 ± 0.0013	P = 0.64
V_E	2.58 ± 0.25	2.40 ± 0.21	P = 0.999998	2.45 ± 0.24	2.65 ± 0.21	P = 0.9998	2.53 ± 0.24	2.92 ± 0.41	P = 0.998
V_{O2}	0.063 ± 0.008	0.055 ± 0.006	P = 0.995	0.063 ± 0.007	0.061 ± 0.005	P = 0.9998	0.064 ± 0.008	0.063 ± 0.006	P = 0.99999999

Supplemental table 1. Vglut2 positive innervations from central noradrenergic neurons to the brain nuclei important in breathing control

Vglut2⁺ noradrenergic nuclei	Downstream target of Vglut2⁺ NA neurons	The role of the downstream target in breathing control	Reference
C1	preBötzinger complex	Generate inspiratory rhythm	Malheiros-Lima et al. (2018)
	parafacial region (pFRG)	Regulate active expiration during chemosensory stimulation	Malheiros-Lima et al. (2020)
	Locus Coeruleus (LC)	Chemosensitive, regulate chemosensation	Abbott et al. (2013); Holloway et al. (2013)
	A5	Inhibitory drive for chemosensation and respiratory rhythm	Abbott et al. (2013); Malheiros-Lima et al. (2022)
	A1, A2	Modulate chemosensation, stabilize respiratory rhythm	Abbott et al. (2013); Holloway et al. (2013)
	Lateral parabrachial nucleus (PBN)	Regulate chemosensation and arousal	Abbott et al. (2013)
	Medullary raphe	Regulate chemosensation and expiration	Abbott et al. (2013)
	Nucleus of the solitary tract (NTS)	Receive input from the carotid bodies (a key center for O_2 chemosensation) and other cardiopulmonary afferents	Abbott et al. (2013)
	Dorsal motor nucleus of the vagus	Control respiration rate, regulate airway tone and defense	Abbott et al. (2013)
	Dorsomedial hypothalamus (DMH) lateral hypothalamic area (LHA)	Modulate baseline respiration, chemosensation, arousal	Abbott et al. (2013)
	Paraventricular thalamic nucleus (PVT)	Regulate arousal	Abbott et al. (2013)
	Paraventricular nucleus (PVN)	Modulate baseline respiration, respiratory response to hypoxia	Abbott et al. (2013)
Locus Coeruleus (LC)	Lateral parabrachial nucleus	Regulate chemosensation and arousal	Yang et al. (2021)